2010

Evaluation of high-latitude boreal forest growth using satellite-derived vegetation indices

Logan T. Berner
Western Washington University

EVALUATION OF HIGH-LATITUDE BOREAL FOREST GROWTH USING SATELLITE-DERIVED VEGETATION INDICES

By

Logan T. Berner

Accepted in Partial Completion

of the Requirements for the Degree

Master of Science

_____

Moheb A. Ghali, Dean of the Graduate School

ADVISORY COMMITTEE

_____

Chair, Dr. Andrew G. Bunn

_____

Dr. David O. Wallin

_____

Dr. David U. Hooper

MASTER'S THESIS

In presenting this thesis in partial fulfillment of the requirements for a master's degree at Western Washington University, I grant Western Washington University the non-exclusive royalty-free right to archive, reproduce, distribute, and display the thesis in any and all forms, including electronic format, via any digital library mechanisms maintained at WWU.

I represent and warrant this is my original work, and does not infringe or violate any rights of others. I warrant that I have obtained written permission from the owner of any third party copyrighted material included in these files.

I acknowledge that I retain ownership rights to the copyright of this work, including but not limited to the right to use all or part of this work in future works, such as articles or books.

Library users are granted permission for individual, research and non-commercial reproduction of this work for education purposes only. Any further digital posting of this document requires specific permission from the author.

Any copying or publication of this thesis for commercial purposes, or for financial gain, is not allowed without my written permission.

Signature _____

Date _____

EVALUATION OF HIGH-LATITUDE BOREAL FOREST GROWTH USING SATELLITE-DERIVED VEGETATION INDICES

A Thesis

Presented to

The Faculty of

Western Washington University

In Partial Fulfillment

of the Requirements for the Degree

Master of Science

by

Logan T. Berner

April 2010

ABSTRACT

Vegetation in northern high-latitudes plays an important role in energy exchange and carbon dynamics, thereby influencing regional and global climate. Vegetation indices derived from the space-borne Advanced Very High Resolution Radiometers (AVHRR) have suggested decreased photosynthetic activity during recent decades within some continental regions of the pan-arctic boreal forests. The purpose of this research was to determine associations between the normalized difference vegetation index (NDVI), as derived by both AVHRR and Moderate Resolution Imaging Spectroradiometers (MODIS), and inter-annual variations in radial stem growth in high-latitude coniferous forests. During 2008 and 2009, tree core samples were collected at 12 sites in northeast Russia and at 10 sites in northwest Canada. Ring-width indices (RWI; n = 27) were generated for larch, spruce, and pine genera and these were correlated with summer NDVI derived from the AVHRR sensors over the 1982 to 2008 period. The correlations between NDVI and RWI were then examined between 2000 and 2008 using both MODIS and AVHRR. The sensors showed similar abilities to proxy radial growth and NDVI-RWI correlations appeared mostly insensitive to changes in MODIS grain sizes between 250 m and 24 km. Over the 27 year period RWI and NDVI showed positive, though variable, correlations ($r = 0.43 \pm 0.19$, $n = 27$**)**. For pine and spruce, both evergreen conifers, the annual rate of radial growth was significantly correlated with growth during previous years, as was canopy development, as proxied by NDVI. Larch, however, did not show year to year persistence in either radial growth or canopy development, a finding that points to differences in growth patterns between functionally-distinct tree genera. These findings suggest that negative trends in NDVI may reflect decreased radial growth at some locations and that attempts to model tree growth and carbon uptake using NDVI need to take into account multi-year persistence in tree growth. Additionally, the work shows similarities between AVHRR and MODIS, suggesting potential to bridge the historical AVHRR record with the newer and finer resolution MODIS record.

ACKNOWLEDGEMENTS

There are many people who helped make this research possible. I would first like to thank my graduate advisor Dr. Andy Bunn for all of his unfaltering support and tireless mentoring efforts. I would also like to thank the members of my graduate research committee, Drs. David Wallin and David Hooper, for their valuable advice and suggestions. Drs. Andrea Lloyd, Pieter Beck, and Scot Goetz all contributed in various and much appreciated manners to the creation of this body of work. Chris Robertson and Alex Westcott assisted with field work in Canada, while Alexander Zhulidov and Anatoly Nikolaev provided field assistance in Siberia. Tom Quinn at CH2MHill Polar Services helped with organizing the Russian and Canadian field logistics. Jody Gertz, Holly Faulstich and Max Janicek assisted with tree core processing. Funding for this research was provided by the National Science Foundation (ARC-0612346 to AHL and AGB).

TABLE OF CONTENTS **Page**

LIST OF FIGURES AND TABLES

Figures

Tables

1. INTRODUCTION

1.1. **Northern High-Latitudes, Carbon and Climate**

The Arctic and boreal forest biomes together cover roughly 30% of the combined Eurasian and North American landmass (~ 25 million km^2 above 50° N), accounting for approximately 12% of annual global vegetation productivity during recent decades [Kimball et al., 2006]. Northern high-latitude biomes play an important role in regulating regional and global climate through energy partitioning and carbon storage [Chapin et al., 2000, 2005; Vygodskaya et al., 2007]. The region has experienced large changes in permafrost extent and vegetation since the onset of the Holocene, ~ 10,000 years before present. Currently the southern extent of discontinuous permafrost in North America occurs between 50° and 60° N, except for some mountainous areas further south, while in Europe it is found only in high mountain areas and the northern most parts of Norway, around 60° N [Brown et al., 1997]. At the end of the last ice age, permafrost extended to around 45° N in Europe and 40° N in North America, storing large pools of organic carbon locked away in perennially-frozen soils [Zimov et al., 2006]. Recent work suggests that approximately 1672 Pg of organic carbon, representing an estimated 50% of the global below ground organic carbon pool, is stored within the northern circumpolar permafrost soils [Tarnocai et al., 2009]. Much of this organic carbon is stored in yedoma deposits found in Alaska and Siberia where wind-blown glacial dust fostered mammoth steppe-tundra ecosystems during the Pleistocene. Thawing of yedoma-like soils in Europe and Western Siberia during the Holocene may have released 500 Pg of carbon, contributing to the increase in atmospheric carbon from ~360 Pg during the last glacial maximum to ~560 Pg during preindustrial times [Zimov et al., 2006].

Since the industrial revolution the atmospheric carbon pool has increased to ~730 Pg [Zimov et al., 2006], from 280 ppm to 379 ppm in 2005 [Intergovernmental Panel on Climate Change (IPCC), 2007]. While CO_2 is one of many greenhouse gasses generated by natural and anthropogenic processes, its contribution of $+1.66 \pm 0.17$ W m^{-2} to radiative forcing since pre-industrial times is larger than any other gas [IPCC, 2007]. Though the global mean atmospheric temperature rose

approximately 0.74°C ± 0.18°C over the past century [IPCC, 2007], much of the Arctic warmed 2°-3°C over the same period with the most pronounced warming occurring during winter and spring [Arctic Climate Impact Assessment (ACIA), 2004]. In a 2000-year, multi-proxy reconstruction of pan-arctic temperatures, Kaufman et al. [2009] found a pervasive cooling trend (-0.22°C ± 0.06°C per 10^3 yrs) during the period associated with reduced summer insolation driven by orbital changes. The reconstruction also showed that four of the five warmest decades occurred between 1950 and 2000, with the 1999-2008 10-year interval being the warmest during the past 2000 years, in spite of model simulations predicting continued reductions in summer insolation through the 20th century due to orbital forcing. Warming-induced reductions in snow and ice extent, as well as changes in tree and shrub extent, can further amplify regional heating [Chapin et al., 2005].

Many physical and ecological processes at high-latitudes occur near the freezing point of water and thus changes in temperature or water regimes can act as a climate feedback [Chapin et al., 2005]. Over the past century much of the permafrost in Alaska, western Canada, and eastern Siberia has warmed 2°-4°C, which in Alaska has left the remaining discontinuous permafrost within 1-2°C of thawing [Osterkamp et al., 2000; Romanovsky et al., 2007; Burn and Kokelj, 2009]. Thermokarst formations occur in permafrost when underlying ice-lenses and wedges melt, thereby causing a loss of structural integrity resulting in surface subsidence and, frequently, inundation. Inundation can cause conversion of forests to wet meadows, bogs, and lakes that are quickly colonized by grasses, sedges, horsetails, and algae [Osterkamp et al., 2000], thereby altering the land surface surface albedo and acting as a potential source of microbially-mediated methane production [Zimov et al., 1997]. Changes in surface temperature and precipitation can also affect wild fire activity, insect out breaks, and other vegetation disturbances (e.g. frost kills), thereby inducing increased carbon emissions from terrestrial sources and causing changes in surface albedo, both potential feedbacks to changing climate regimes [Chapin et al., 2000].

Changes in temperature and water have had a number of effects on vegetation, including

changes in the distribution, composition and productivity of forest and tundra communities. Shrub expansion in to the tundra [Tape et al., 2006], northern advancement of tree line [Lescop-Sinclair and Payette, 1995; Devi et al., 2008], and succession from lichen to vascular plants [Olthof et al., 2008, 2010] have all been documented. In a study of Siberian larch (*Larix siberica*) near tree line in the Polar Urals, researchers found that in addition to tree line advancing into the tundra during the previous century, the growth form of *L. siberica* had changed significantly since the 15th century [Devi et al., 2008]. Between the 15th and early 20th centuries *L. siberica* assumed a low profile, creeping form, though during the early part of the 20th century it started showing multi-stem vertical growth. Since the 1950s, 90% of trees in their study area showed single-stemmed growth forms and a marked increase in biomass production. Increased biomass production between 1981 and 2008 has also been observed in bryophyte and evergreen shrub communities in the Canadian High Arctic [Hudson and Henry, 2009].

While much of the pan-arctic tundra and tundra-taiga boundary have shown increased productivity in recent decades, the boreal forests have generally shown stagnant or negative trends in productivity during this period [Angert et al., 2005; Goetz et al., 2005; Bunn et al., 2006]. Evidence from tree-rings, satellites and stable isotopes suggests that warmer and drier summers are inducing temperature and or drought-related stress, thereby causing reductions in forest growth within some regions [Barber et al., 2000; Lloyd and Fastie, 2002; Lloyd and Bunn, 2007; Zhang et al., 2007, 2008]. In a circumpolar analysis of boreal forest growth, Lloyd and Bunn [2007] found that the frequency of inverse correlations between tree growth and temperature increased after 1942, while the frequency of positive correlations declined during this period. Additionally, the researchers found that negative correlations between tree growth and temperature were more prevalent in the warmer and drier parts of species' ranges. Using satellite-derived measurements, Angert et al. [2005] showed negative trends in vegetation production—browning—in most of the North American and Eurasian high-latitude forests between 1994 and 2002, with the exception of some of the coldest continental

areas in which increased vegetation productivity—greening—corresponded to warming temperature trends. The browning trends were partially explained by more negative (drier) Palmer Drought Indices in these regions. Zhang et al. [2008] further demonstrated, through the use of satellite-based vegetation modeling, that pan-arctic net primary productivity (NPP)—the mass of C fixed per unit area and time minus autotrophic respiration costs—between 1983 and 2005 showed, on the whole, decreased temperature constraints and increased moisture limitations. While warming in recent decades has induced increased productivity in some regions, notably the tundra, higher temperatures and drier summers appear to be causing reduced productivity in large tracks of pan-arctic boreal forest.

Changes in boreal forest productivity associated with a warming and drying climate may reduce carbon uptake and increase emissions due to increased frequency and severity of disturbance events (e.g. fires and insects). Changes in carbon cycling and energy partitioning within these forested regions may have large feedbacks on climate, thus making this an important field of study. Understanding the potentially mixed and complex responses of high latitude forests to climate change will require observational and experimental studies conducted over a range of spatiotemporal scales.

1.2. **Space-borne Vegetation Monitoring**

Remote sensing will play an important role in the assessment of the spatial and temporal changes in vegetation and other land surface features which may affect climate. Across the literature, satellite-derived indices of key ecosystem processes (e.g., productivity) have been increasingly used to augment site-based studies and provide more spatially complete records of ecosystem change [see ACIA 2004; McGuire et al., 2009]. Since the 1980s satellites have been used to monitor vegetation activity across the planet, with the most widely used metric being the normalized difference vegetation index [NDVI; Tucker, 1979]. The index is calculated as the normalized ratio of

reflectance in near-infrared (~ 1 μm) and red (~ 0.6 μm) wavelengths,

$$NDVI = (\rho NIR - \rho RED)/(\rho NIR + \rho RED) \quad (1)$$

where ρNIR is radiance at near-infrared and ρRED is radiance in red. Theoretical values range between -1 and 1. The index correlates strongly with LAI and the fraction of absorbed photosynthetically active radiation [FAPAR ; Prince et al., 1995]. The index has direct application to, among other things, the dynamic management of forest stands, wildfires, grazing livestock, agricultural harvests, and epidemiological investigations [Running et al. 2004]. Early uses included monitoring the exchange of carbon dioxide between the atmosphere and boreal forests [D'Arrigo et al., 1987], as well as monitoring ephemeral habitat of breeding birds in sub-Saharan Africa [Wallin et al., 1992]. NDVI has been widely used to monitor high-latitude vegetation dynamics [Myneni et al., 1997; Zhou et al., 2001] where it has frequently been coupled with meteorological data to drive models of vegetation productivity [Angert et al., 2005; Bunn et al., 2007; Zhang et al., 2008].

Models of vegetation productivity generally fall into three major categories. There are models that rely primarily upon satellite observations, models that use prescribed vegetation structure, and models that simulate both carbon fluxes and vegetation structure [Cramer et al., 1999]. Production efficiency modeling (PEM) falls under the first category and is a geospatial technique developed in the last two decades which attempts to model vegetation productivity using satellite-derived vegetation indices, meteorological data, and knowledge of plant physiology. The method works on the theory that a relationship exists between absorbed radiation and rates of photosynthetic carbon uptake [Running et al., 2004]. The models employ the concept of light use efficiency (LUE) which biologically is a term that describes the efficiency with which a plant is able to convert absorbed electromagnetic energy into biomass [McCallum et al., 2009]. LUE varies across species and through time, with herbaceous vegetation generally showing values from 1.0 – 1.8 g C MJ^{-1} and woody plants exhibiting efficiencies between 0.2 – 1.5 g C MJ^{-1} [Running et al., 2000]. The range in values arises principally from differences in maintenance respiration costs and suboptimal climatic

conditions [Running et al., 2000]. This modeling technique uses environmental constraints to reduce the LUE below a theoretical maximum and then uses levels of incident and absorbed radiation to simulate energy to carbon conversion.

In a review of PEM techniques, McCallum et al. [2009] noted that the models take the general form

$$GPP = PAR*FAPAR*LUE*Scalars \quad (2)$$
$$NPP = GPP - Ra \quad (3)$$

where:

GPP	Gross Primary Productivity (g C m^{-2})
PAR	Photosynthetically Active Radiation (MJ m^{-2})
FAPAR	Fraction of Absorbed PAR (dimensionless %)
LUE	Light Use Efficiency (g C MJ^{-1})
Scalars	Temperature, (VPD) Vapour Pressure Deficit, etc (0-1)
NPP	Net Primary Productivity (g C m^{-2})
Ra	Autotrophic Respiration (g C m^{-2})

In Equation 2, GPP is modeled at pre-defined time steps using terms describing incident radiation, absorbed radiation, and energy to carbon conversion efficiency which is dependent on environmental limitations. Autotrophic respiration—carbon use related to plant growth, maintenance, and ion uptake—is then subtracted from GPP to yield estimate of NPP over a given period (Equation 3). FAPAR is generally proxied either directly, or in a slightly modified form, by NDVI and is considered an integrator of climatic conditions owing to the affect of water availability, temperature and cloudiness on leaf form and function [Schloss et al., 1999]. While NDVI is coupled with incident radiation to determine the amount of energy that is absorbed, the models employ scalars to change the LUE depending on environmental constraints.

Determination of LUE and environmental constraints can vary widely between models. The Global Production Efficiency Model (GLO-PEM), for instance, was one of the first PEMs and took the approach of classifying vegetation LUE based on C3 or C4 metabolic pathways [Prince and Goward, 1995]. In this model FAPAR was calculated using NDVI data from AVHRR. Running et al.

[2004] developed a PEM driven by MODIS NDVI, though used a different technique for determining LUE. The MODIS model first defined seven biome types reflecting differences in biophysical and biogeochemical characteristics. Differences in physical structure that drive changes in air and soil temperatures, as well as water availability, may influence rates of nutrient processing and thus the overall efficiency of energy-carbon conversion. Additionally, biome classes may exhibit marked differences in how plants store and process carbon and other nutrients. Biome-BGC, an ecophysioloical mechanistic model of water and nutrient fluxes, was used to simulate LUE for each biome class [Running and Hunt, 1993]. In each model, LUE was systematically reduced from the theoretical maximum based on air temperature and vapor pressure deficit (VPD) constraints. The MODIS model truncated carbon fixation when temperatures fell below 0°C or when VPD exceeded 20 hPa, reflecting, respectively, inhibition of carbon fixation due to ice formation over leaf stomata and physiological responses to minimize water loss. While differences arise in precisely how PEMs are executed, the models show similarities in overall form.

Satellite-driven PEMs are useful for gleaning an understanding of the spatial dynamics of vegetation activity; however, the relatively short data records preclude conducting rigorous time series analyses for all but a few satellites. The AVHRR record, now spanning nearly 30 continuous years of operation, is one of the few space-borne sensors with a long enough record to permit studies of vegetation changes through time. Using AVHRR-derived NDVI to drive PEMs simulating vegetation productivity, researchers have shown that from the 1980s through the early 1990s boreal forest and tundra ecosystems generally showed increased productivity [Myneni et al., 1997; Jia et al., 2003; Angert et al., 2005]. Trend analyses covering the 1990s through mid 2000s found continued greening throughout much of the pan-arctic tundra, but negative or no trends in boreal forest productivity. Inland continental forests in particular were found to show browning trends during this period [Angert et al., 2005; Goetz et al., 2005; Bunn and Goetz, 2006]. While these satellite-based models showed decreased productivity within large tracks of boreal forest, it is important to verity

the model results using field measurements of biophysical parameters.

Verifying and characterizing PEM estimates of NPP in boreal forests is particularly important given recent findings showing reduced growth in many regions. Past efforts have attempted to link satellite-based NPP estimates with biomass harvests, CO_2 flask and eddy covariance flux tower measurements (Running et al., 2004). Biomass harvests encompassing the footprint of a coarse spatial resolution model are generally not feasible, while both flask and flux tower measurements of CO_2 are hindered by not known the 'footprint' represented by the samples. Comparison of NPP estimates with tree ring data may be a means by which to validate observed browning trends.

Ring width relates closely to annual tree biomass production and C sequestration, while the distinct annual growth rings permit retrospective analysis of forest productivity [Graumlich et al., 1989; Bascietto et al., 2004; Bouriaud et al., 2005]. Malmstrom et al., [1997] previously demonstrated a significant relationship between a NDVI-based model of NPP and ring width indices from a mixed *Picea glauca* and *Betula papyrifera* stand in Alaska, while Lopanis et al., [2004] showed a positive relationship between NDVI and ring width measurements from *Pinus sylvestris* and *Picea obovata* in eastern Russia. Unfortunately, many of the tree ring records publically-available through the NOAA International Tree-Ring Data Bank (ITRDB; ncdc.noaa.gov) were collected prior to the mid 1990s. As a result, there are relatively few available tree ring records collected at northern high latitudes in recent years against which NDVI, or modeled NPP, can be compared. As tree rings appear a potentially viable means by which to verify observed browning trends in high latitude forests, it is important that an effort be made to update the tree ring chronologies so as to increase the period of overlap between satellite data and measurements of tree growth.

1.3. **Scope of Research**

The goal of this research was to examine the interannual relationship between NDVI and tree stem growth in an effort to ground truth NDVI-based model results suggesting decreased productivity in forest growth at some high latitude locations. To this end I sought to assess the extent to which the NASA Global Inventory Modeling and Mapping Studies [GIMMS; Tucket et al., 2005] NDVI dataset, derived from the NOAA Advanced Very High Resolution Radiometers (AVHRR), reflected stand-level cambial growth at selected sites in Canada and Russia between 60° and 70°N. The GIMMS data set extends from 1981 through present and was chosen because it has one of the longest, best-documented and continuous records and has been widely used for monitoring boreal and arctic vegetation dynamics [e.g. Myneni et al., 1997; Goetz et al., 2005; Bunn and Goetz, 2006]. As the AVHRR sensors were originally designed for meteorological applications, not vegetation monitoring, I also sought to compare the ability of GIMMS to proxy forest growth with that of the newer Moderate Resolution Imaging Spectroradiometer (MODIS) launched in 2000. MODIS has been optimized for terrestrial vegetation monitoring and is considered a successor of the AVHRR system with improved spectral, radiometric and spatial characteristics [Ji et al., 2008]. Comparing NDVI and tree growth across sensors and spatial scales helps to both improve our ability to interpret trends in NDVI over forested regions and refine our ability to model and monitor carbon dynamics at high-latitudes using remote sensing techniques.

1.4. **Objectives**

The purpose of this research was to assess the extent to which NDVI can proxy forest growth at selected sites in the northern high-latitudes. To this end, I sought to:

1. Examine the relationship between stand-level cambial growth patterns and AVHRR-derived measurements of NDVI between 1982 and 2008.
    a. Examine correlations between NDVI and indices of tree growth for spruce, pine, and

larch

b. Contrast NDVI and tree growth autocorrelation patterns between evergreen and deciduous conifers

2. Conduct a cross-sensor and cross-scale comparison of the relationship between stand-level cambial growth patterns and vegetation indices derived from MODIS and AVHRR sensors.
    a. Compare NDVI-tree growth correlations for NDVI derived from MODIS and AVHRR at 8 km and 24 km resolutions
    b. Compare NDVI-tree growth correlations for NDVI derived from MODIS at 250 m, 750 m, 8 km, and 24 km resolutions.

The first objective is the subject of chapter three, while the second is covered in chapter four.

2. STUDY AREAS

2.1. **Site Selection**

During the summers of 2008 and 2009, tree cores were collected from 22 sites in the high latitude (60°-70° N) forests of Russia (n = 12) and Canada (n = 10; Figure 1, Table 1). Samples were collected along the Lena River in central Siberia, the Kolyma River in northeastern Siberia, and near Great Slave Lake in the McKenzie River Basin of the Canadian Northwest Territories. Field work took place out of the towns of Yakutsk and Zhigansk along the Lena, Cherskii along the Kolyma, and Yellowknife in Canada.

These regions were selected in part to help fill gaps in the tree ring data available through the NOAA ITRDB and also to update high latitude tree ring chronologies, many of which were originally collected during the early 1990s and thus have minimal overlap with satellite data. Additionally, little work has been conducted at high latitudes relating satellite-derived vegetation indices to biophysical vegetation characteristics. As the purpose of this study was to investigate the relationship between tree growth and vegetation indices, an effort was made to select sites where

forest composition and potential growth patterns would be similar over tens of kilometers. The sites in Russia were selected with the help of knowledgeable local scientists and guided heavily by logistical constraints. In Canada, site selection was less constrained by logistical considerations and thus forest density information [Hansen et al., 2003] and Google Earth were used to select accessible sites showing greening or browning trends in NDVI between 1982 and 2003, as reported by Bunn and Goetz [2006].

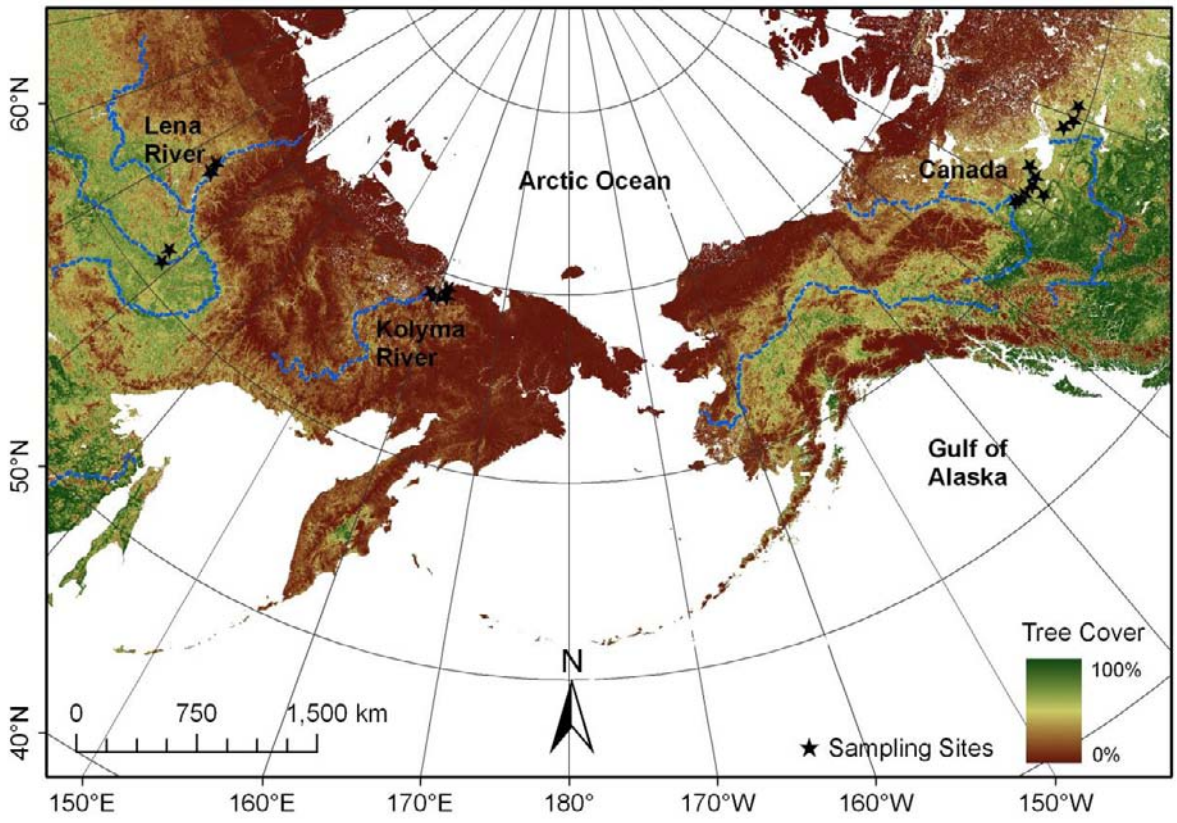

Figure 1. Map of eastern Eurasia and western North America showing the location of tree core sampling sites (n = 22). Samples were collected along the Lena and Kolyma Rivers in Siberia, as well as near Great Slave Lake in Canada. The tree cover data are from Hansen et al. [2003].

Table 1. Location and taxa of the tree samples collected at 22 sites in Russia and Canada.

Genus	Species	Common Name	Site	Latitude	Longitude	N Trees	Tree Cover (%) [a]
Larix	*gmelinii*	Dahurian larch	CHE	68.74804	161.42429	57	12
			DVN	68.66941	159.07575	9	10
			GRS	68.74863	161.37798	13	12
			IND	66.27584	123.91683	25	25
			PAR	68.53253	160.19837	13	12
			ROD	68.72746	161.55157	14	11
			SYL	66.21044	124.00488	24	26
			TRL	69.20078	161.44083	7	9
			YUT	62.02985	128.59393	30	41
			ZHG	66.75067	123.41649	60	25
Picea	*glauca*	white spruce	BIS	61.69122	-116.94424	10	43
			FAL	61.19368	-119.99229	8	50
			NML	60.32040	-119.04956	21	49
	mariana	black spruce	DAR	60.90921	-111.59396	10	29
			ELF	61.35397	-120.80107	5	48
			FAH	61.43301	-121.26761	19	53
			SQT	61.09494	-118.78281	22	32
			TAL	60.55464	-110.60712	8	39
	obovata	Siberian spruce	IND	66.27584	123.91683	8	25
			ZHF	66.76183	123.34979	10	24
Pinus	*banksiana*	jack pine	DAR	60.90921	-111.59396	14	29
			ELF	61.35397	-120.80107	16	48
			FAL	61.19368	-119.99229	10	50
			MAR	60.55650	-109.03765	23	34
			MKZ	61.13348	-117.80937	18	45
			TAL	60.55464	-110.60712	14	39
	sylvestris	scots pine	BAL	61.34005	129.08442	31	42

[a] Tree cover data from Hansen et al. [2003].

2.2. **Canada**

The Canadian study area near Great Slave Lake is composed of eastern Taiga Plains and Taiga Shield ecozones, as identified by Environment Canada [Ecological Stratification Working Group (ESWG), 1995). Winter temperatures average -21°C, with mean summer temperature of approximately 12°C.

Since the 1950s, mean annual air temperatures have increased 1°-3°C, with climate models suggesting a potential 3°-5°C increase during the coming century [ACIA, 2004]. Annual precipitation ranges from 250 to 400 mm, with models showing annual precipitation increasing approximately 20% by 2099 [ESWG, 1995; IPCC, 2007]. The physical landscape includes broad expanses of glacial-till lowlands incised with rivers channels and overlain with wetlands. Much of the region is underlain by permafrost which promotes seasonal overland surface seepage and wetland development. Forest cover consists of mixed-wood forests of close-canopy black spruce (*Picea mariana*), white spruce (*Picea glauca*), and jack pine (*Pinus banksiana*) occurring in some cases with tamarack (*Larix laricina*), birch (*Betula spp.)* and aspen (*Poplar spp.*). The understories are frequently composed of feathermoss (*Pleurozium schreberi*), bog cranberry (*Oxycoccos palustris*), blueberry (*Vaccinium spp*.) and various lichen and sedges [ESWG, 1995].

2.3. **Russia**

The Lena and Kolyma Rivers drain the Russian republic of Yakutia into the Laptev and East Siberian Seas, respectively. There is a paucity of climate data for the region; however, Esper et al. [2009] reported that the mean June through August station-based air temperature over the 1951-1980 period was 15.2°C in Eastern Siberia and had an annual range of 57°C. Temperature reconstructions along a N-S transect in central Yakutia found mean regional surface warming of +0.29°C per decade [Romanovsky et al,. 2007], while climate models predict an additional 3°-4°C warming of mean annual temperature by the end of the 21st century [ACIA, 2004]. Annual precipitation across the region varies widely, from 350 mm to 700 mm, and is expected to increase by 15% to 20% by 2099 [Berezovskaya et al., 2004; IPCC, 2007]. The region is underlain by continuous permafrost and in the areas sampled has little topographic relief. Forest composition along the Lena River is primarily Dahurian larch (*Larix gmelinii*) with occasional Scots pine (*Pinus sylvestris*) and Siberian spruce (*Picea obovata*). Tree cover along the northern Kolyma River is restricted to *Larix gmelinii* with

extensive dwarf birch understories. In both areas Labrador tea (*Ledum spp*.), willows (*Salix spp.),* moss and lichens are common. Russian scientists identify two separate species of larch, *L. gmelinii* and *L. cajanderi*; however, *L. cajanderi* is not generally recognized as a separate species in most English-language journals and thus all larch samples were called *L. gmelinii*.

3. HIGH-LATITUDE TREE GROWTH AND NDVI

3.1. **Background Information**

Past work has shown a correlation between variations in NDVI from 50°-80° N and seasonal changes in atmospheric CO_2 drawdown at Point Barrow, along the north coast of Alaska, thus demonstrating a measurable link between terrestrial vegetation and seasonal variations in atmospheric CO_2 [Tucker et al., 1986]. Following upon this work, D'Arrigo et al. [1987] examined CO_2 drawdown at Point Barrow in relation to four *P. glacua* tree ring chronologies from across the North American tree line and NDVI from areas in North America and Eurasia classified as boreal forest. The tree ring indices were significantly correlated with the amplitude of annual CO_2 drawdown between 1971 and 1982 and the NDVI-driven model suggested that the high latitude forests contributed to ~ 50% of the mean seasonal CO_2 amplitude in Barrow and ~ 30% to the more globally-representative Mauna Loa, Hawaii, CO_2 measurements. These studies together demonstrate a measurable link between space-borne vegetation measurements, high-latitude tree growth and global atmosphere-biosphere CO_2 exchange.

In more recent years attention has gone into examining the relationship between NDVI, or NDVI-driven PEMs, and different measurements of tree growth. Linking NDVI to measureable biophysical characteristics or states permits a more robust interpretation of NDVI trends and patterns. Maximum late wood density at two *P. glacua* sites in Alaska and one *L. gmelinii* site in Russia were positively correlated with modeled NPP, as was a combined spruce-birch ring-width chronology [D'Arrigo et al., 2000]. Over a 9 year period, Wang et al. [2004] showed very strong

correlations between NDVI during the growing season and tree diameter growth, foliage production, and seed production within an oak forest (*Quercus spp.*) in Kansas. Along a five-site transect from southern taiga to tundra in the Komi Republic in central Russia, tree ring indices and integrated June-August NDVI were significantly correlated for *P. siberica* and *P. sylvestris* [Lopatin et al., 2006]. These studies further demonstrated links between NDVI and various facets of tree growth.

In these studies, NDVI was selected from particular months during summer or over the entire growing season. Kaufmann et al. [2004] examined the relationship between tree ring width indices at 48 mid to high-latitude sites, mostly concentrated in Alaska, and NDVI derived monthly from April through October. Significant relations were found between tree growth and NDVI during June and July only. Additionally, the researchers suggested no causal relationship between NDVI and tree rings, but instead that they share a common signal imparted by a common causal variable such as NPP , which reflects the amount of energy available to the tree to produce leaves and increase biomass, essentially what NDVI and tree rings proxy. The goal of this research was to assess the extent to which the GIMMS NDVI dataset reflects stand-level cambial growth over a range of high-latitude forest sites. A new algorithm for defining the NDVI growing season both spatially and temporally was also employed.

3.2. **Data and Methods**

3.2.1. Tree Core Sampling

Tree cores at 22 sites, each covering a few hectares, were sampled between 2008 and 2009. At each site, 15 to 60 straight, canopy-dominant conifers free from visible signs of damage were selected. An attempt was made to sample across canopy-influencing age classes and to find trees representative of those in the surrounding area. In Canada, *P. banksiana, P. mariana,* and *P. glauca* were sampled, while in Siberia samples were taken from *L. gmelinii, P. sylvestris*, and *P. siberica*. Two perpendicular cores were extracted at roughly breast height (~0.8 to 1.3 m above ground) from each

tree using 5 mm increment borers. Two cores were taken from each tree so as to help account for potential directional differences in growth, though an effort was made to select circular trees. The diameter at breast height and estimated distance to the nearest neighbor of comparable size were recorded for each tree. The canopy and general understory compositions were recorded. Digital photographs were taken at each site and a global positioning system was used to determine the coordinates associated with the approximate center of each stand.

3.2.2. Tree Core Processing

In the laboratory the tree cores were mounted, sanded and visually cross-dated using standard dendrochronological procedures [Pilcher, 1990]. Annual growth rings were measured to the nearest micrometer using an Olympus SZ61 stereo microscope equipped with a UniSlide linear encoder measuring system (Velmex, Inc., Bloomfield, NY). After measuring, the cross-dating accuracy of each series was verified statistically using a combination of the COFECHA software and the dplR package in R [Holmes, 1983; Bunn, 2008, in press]. Series found not to properly cross-date were visually examined for missing growth rings. If possible, the location of missing rings was deduced by comparing the series with the second core from the tree or with others from the stand. If the location could not be determined, then the series was excluded from the chronology.

The series were subsetted after cross-dating to include only measurements from 1981 through 2007 or 2008, depending on the final full year of growth. Growth measurements from each tree were divided by the series mean and stand-level ring-width index (RWI) chronologies were created by averaging together each standardized series. Construction of stand-level chronologies helps to remove the variability in growth experienced by individual trees owing to factors such as competition and damage while retaining the common growth signal [Biondi, 1999]. A total of 499 trees (915 cores) were included in the analysis. It was not always possible to measure or cross date a core due to missing pieces or extreme suppression of growth. While 17 of the 22 stands were single-

species dominant, five stands exhibited co-dominance of tree species. This occurred once in Siberia with a mixed *L. gmelinii* and *P. siberica* stand and at four of the Canadian sites with mixed *P. banksiana* and *P. mariana* stands. In these cases separate chronologies were created for each species, for a total of 27 chronologies against which NDVI was compared. Appendix one provides more detailed information the tree ring chronologies. All tree ring data used in this analysis will be made publicly available online through the ITRDB.

3.2.3. AVHRR Vegetation Index

The GIMMS NDVI dataset (Version G) from 1982 to 2008 was used in this study [landcover.org; Tucker et al., 2005]. The data were derived from measurements by the AVHRR sensor channels one and two, which respectively resolve regions of the spectrum at red (0.58-0.68μm) and near-infrared (0.725-1.00 μm) wavelengths. The sensors are carried by the afternoon-viewing NOAA satellite series (NOAA 7, 9, 11, 14, 16, and 17). Data processing includes corrections for atmospheric aerosols, effects from the El Chichón and Pinatubo eruptions, solar zenith angle effects, and sensor differences and degradation [Tucker et al., 2005]. GIMMS provides 24 global NDVI images per year, with the first image of each month representing the month's first 15 days, and the other image the remainder, at a spatial resolution of 8 km and a spatial accuracy of ± 1 pixel.

The growing season NDVI was calculated on a pixel-by-pixel basis for each year over the 1982 to 2008 period. A pixel-based growing season definition was used because the timing of vegetation green-up and senescence can vary widely in boreal regions [Beck et al., 2007]. This method helps to ensure that NDVI was measured during periods of similar vegetation phenology. Determination of the growing season was a two step process. The MODIS Land Cover Dynamics product [MOD12; Zhang, 2003] was used to determine the latest date between 2001 and 2004 at which NDVI during spring began to increase and the earliest date at which the index stopped decreasing at the end of autumn. The length of time between the two dates was considered to be the

growing season length. The growing season length was calculated using 30 arcsecond data (~1 km at equator) and these data were averaged over a 64 km^2 area to determine the mean growing season length for each GIMMS-NDVI pixel. For each pixel, the growing season length remained invariant among years. Growing season NDVI was determined by selecting the highest value output from a time-series moving average with window length equivalent to the growing season length (Figure 2). This approach helps account for spatial and temporal differences in the timing of vegetation green-up and senescence, which are large in boreal regions [Beck et al., 2007].

The NDVI data and sampling site coordinates were coregistered to a common datum (World Geodetic Society 1984). A land mask based off of the Global Land Cover 2000 database was applied [European Commission Joint Research Center, 2003]. A 3x3 pixel window (~576 km^2) was centered on each sampling site and the mean NDVI within each window was determined for each annual growing season. The window approach helps to accommodate errors in the spatial accuracy of the GIMMS data set and minimize the effect of tree-ring sites being located near pixel margins.

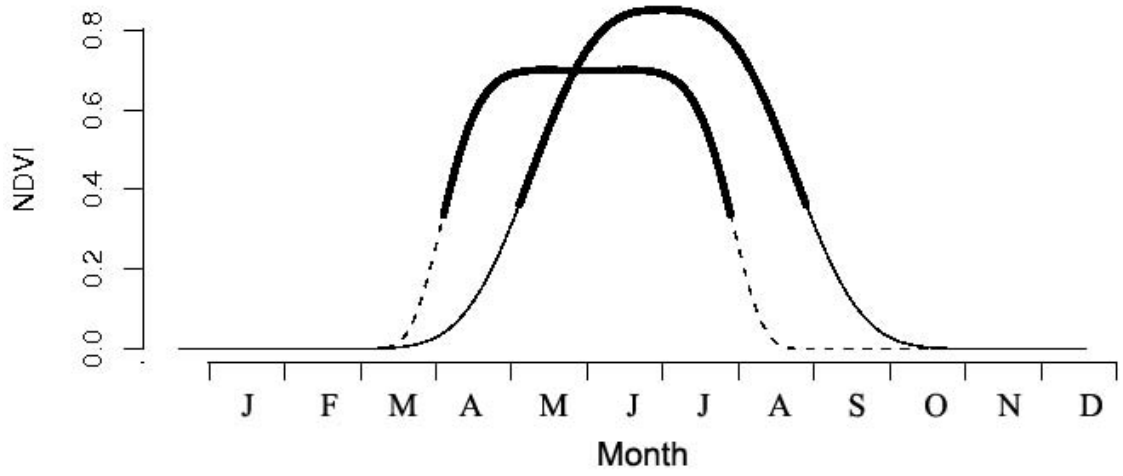

Figure 2. Hypothetical NDVI series for a pixel in two different years. The mean growing season length, n, was estimated from the Land Cover Dynamics product derived from MODIS data. Mean growing season NDVI was calculated for each year from the n continuous NDVI observations (bold line) that generated the highest mean (Figure and calculation courtesy of Pieter Beck, Woods Hole Research Center).

3.2.4. Statistical Analyses

All statistical analyses were conducted using R [R Core Development Team, 2009]. Correlations between RWI and NDVI across years and within sites were determined using Pearson's correlation analyses. Correlation analyses assume statistical independence between samples, which was evaluated by calculating the autocorrelation within each RWI and NDVI series using the dplR package in R [Bunn, 2008, in press]. In instances where significant autocorrelation ($P < 0.05$) was detected at a site the significance value of the NDVI-RWI correlation was penalized by reducing the effective sample size (N_{eff}) in proportion to the strength of the autocorrelation [Dawdy and Matalas,

1964]. Forest stands showing species co-dominance, such as the four *P. mariana* and *P. banksiana* stands sampled in Canada, present a complication when attempting to ascribe NDVI signals to particular genera. The NDVI-RWI correlations, as well as both RWI and NDVI autocorrelations, are presented for three tree genera, though I recognize that the NDVI signal is not exclusive to a particular taxa in mixed-species stands.

3.3. **Results**

3.3.1. NDVI and Tree Growth

Ring-width indices and GIMMS NDVI showed consistent positive associations over the 1982 to 2008 period, except for one *Pinus* site from Canada which displayed a moderately strong negative correlation (Figure 3a; Appendix 2). At a critical value (α) of 0.05, nine of the 27 chronologies were significantly correlated, while at $\alpha = 0.10$, 14 sites were significantly correlated. Penalization of effective sample sizes due to significant autocorrelation in either RWI or NDVI measurements affected seven of ten *Picea* chronologies and five of seven *Pinus* chronologies, thereby reducing the probability of detecting significance at those sites. No *Larix* correlations were penalized due to autocorrelation. Exclusion of the one negative association caused the mean correlation to increase from 0.33 ± 0.46 to 0.43 ± 0.19 (mean ± standard deviation). Mean correlations were 0.38 ± 0.16 for *Larix* ($n = 10$), 0.45 ± 0.19 for *Picea* ($n = 10$), and 0.48 ± 0.24 for *Pinus* ($n = 6$). While mean correlations were slightly higher for *Picea* and *Pinus* in comparison to *Larix*, *Larix* correlations showed lower variability between sites. The strongest correlations observed among NDVI and RWI were 0.67 for *Larix*, 0.75 for *Picea* and 0.82 for *Pinus* stands.

3.3.2. Tree Growth and NDVI Autocorrelation

For each of the three genera included in the analysis, the year to year persistence in annual radial growth and NDVI were investigated by examining the autocorrelation within each dataset. Ring-

width indices for *Pinus* and *Picea* both exhibited significant autocorrelation at lags of one and two years (Figure 3b). Mean correlations at a lag of one year were 0.61 ± 0.26 for *Pinus* and 0.56 ± 0.29 for *Picea*. Interestingly, the NDVI measurements for these two genera also showed similar autocorrelation, with correlation coefficients at a one year lag of 0.52 ± 0.18 and 0.48 ± 0.22 for *Pinus* and *Picea*, respectively. In contrast, neither *Larix* RWI nor NDVI measurements exhibited significant autocorrelation with a mean autocorrelation at a lag of one year of 0.13 ± 0.21 for RWI and 0.16 ± 0.21 for NDVI.

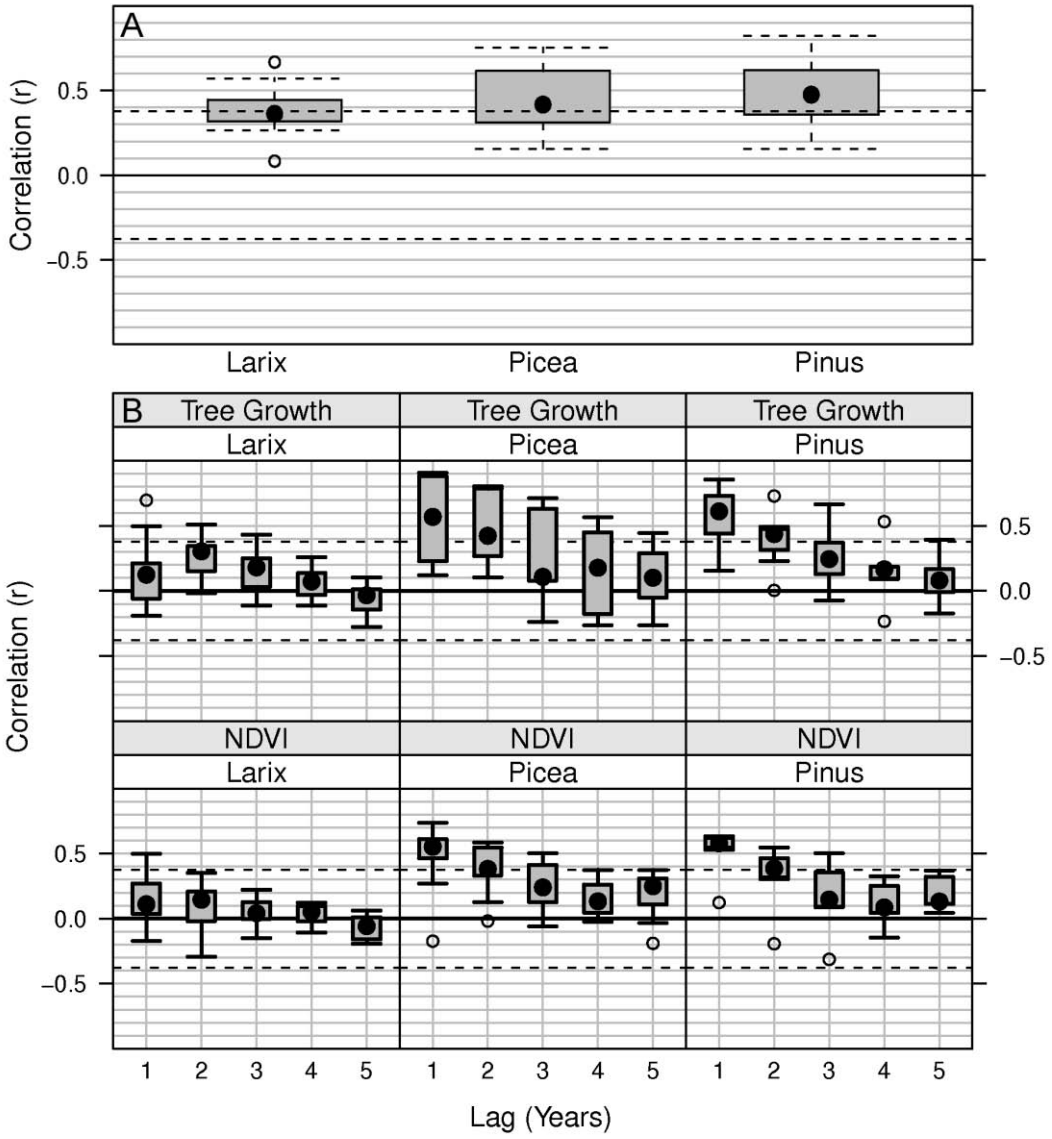

Figure 3. (A) Box and whisker plots showing ring-width and NDVI correlation coefficients for *Larix* (n = 10), *Pinus* (n = 6) and *Picea* (n = 10). Intra-box dots denote medians, box edges denote 25th and 75th percentiles, and whiskers denote 5th and 95th percentiles. Dots represent outliers. One *Pinus* site (FAL) showing a negative correlation was excluded. Dashed lines indicate the r value required for determining correlation significance at p = 0.05 assuming N = 27. See appendix two for N_{eff} and significance values for each site. (B) Box and whisker plots showing ring-width and NDVI autocorrelation by genus.

3.4. **Discussion**

Our findings demonstrate that spaceborne instruments can be used to monitor cambial growth within some forested sites at high-latitudes, though also suggest that it is not a suitable proxy for growth under some circumstances. Past research has demonstrated that, for areas above 40° N, RWI and monthly NDVI are positively related from May through July [Kaufmann et al., 2008]; however, the strongest correlations occur during June and July when NDVI is at its highest [Kaufmann et al., 2004]. Our use of a pixel-based, growing season NDVI capitalizes on these previous findings and yielded stronger correlations between NDVI and RWI than did an analysis using NDVI during June or July, or when NDVI was summed over the June through August period (data not shown). This suggests that our definition of the NDVI growing season helps alleviate the issue of latitudinal and geographical differences between sites in the timing of maximum summer canopy development. As the growing season length was derived from post-2000 MODIS data and held invariant among years, temporal variation in tree-growth related to changes in the length of the growing season since the 1980s will not be captured using this method.

While *Larix*, *Pinus*, and *Picea* are all needle-leaf conifers, *Larix* are different in that they are deciduous, replacing their foliage yearly instead of every three to six years as in the case of many evergreen conifers [Gower et al., 1993]. *Larix* tend to have much higher projected leaf area and foliar nitrogen than evergreen conifers [Gower and Richards, 1990], permitting higher rates of maximum net photosynthesis per unit mass [Gower et al., 1993]. While net primary production rates can be twofold greater for deciduous than evergreen conifers, root production may be half that of evergreens in part because significant energy must be used to frequently replace the N-rich foliage [Gower et al., 2001]. The high energy demand associated with foliage replacement may reduce carbohydrate storage, thereby reducing the trees' ability to buffer radial growth and canopy development during subsequent years in comparison to evergreen conifers. The lack of persistence in RWI and NDVI measurements for *Larix*, compared with significant RWI and NDVI autocorrelation for evergreens,

supports the notion that the persistence of needles can influence carbon storage and subsequent cambial growth [Fritts, 2001]. While RWI autocorrelation is widely known in the field of dendrochronology [e.g. Fritts, 2001], autocorrelation within NDVI measurements, in particular differences in autocorrelation among functionally-distinct tree genera, has not been widely investigated. The autocorrelation patterns provide evidence that forest canopies are contributing to the radiometric signal recorded by AVHRR sensors even in low to moderately forested environments. In spite of evidence of canopy detection, the low to moderate correlations between NDVI and RWI suggest that ring-width is controlled by a variety of factors, potentially spanning many years, and not just by rates of photosynthesis or canopy development [Rocha et al., 2006].

The strength of the correlations between RWI and NDVI are consistent with the discrepancy in scale between cambial cell growth measurements and measurements of landscape properties from spaceborne instruments. The complex mosaic of lakes, bogs, forest-fire remnants and mixed-species forests of varying tree density and age structure hinders the ability of NDVI at a coarse spatial resolution to precisely reflect growth trends of individual species. The magnitude of the NDVI-RWI correlations present here are similar to those reported by Lopatin et al. [2006] who examined the growth of *Picea obovata* and *Pinus sylvestris* at five mixed-species sites in northwestern Russia. Both studies, however, found lower correlations than most of those reported by Wang et al. [2004] who analyzed the relationship between the radial growth of oak trees (*Quercus* spp.) and NDVI in Kansas, U.S.A. Differences in landcover, landscape topography, and canopy architecture may partially account for this discrepancy. Conifers, *Larix* in particular, tend to have lower crown width:height ratios than broadleaf deciduous trees [Gower and Richards, 1990], thus reducing their radiometric influence on satellite imagery acquired from an overhead perspective. Additionally, Wang et al. [2004] used the 1.1 km AVHRR Local Area Coverage data whereas both our work and that of Lopatin et al. [2006] used eight km GIMMS data which were derived from the approximately four km Global Area Coverage data. One *P. banksiana* chronology (FAL) from a mixed-species site

displayed a negative correlation with NDVI, which may have resulted from differences in canopy development between *P. banksiana* and *P. mariana*, interspecific competition within the stands, or an exogenous factor (e.g. insects). These studies support the use of NDVI in monitoring high-latitude forest conditions, although they highlight some biophysical and technical limitations to such an approach.

In spite of mixed-species stands, topographic heterogeneity, and NDVI with a coarse spatial-resolution, our findings demonstrate a coupling between space-based measurements of canopy greenness and cambial cell growth. Global carbon models are partially driven by spectral radiation indices (such as vegetation indices and leaf area indices) using space-based records that cover wide geographic areas but are only a few decades long. Tree ring records are spatially-limited but span centennial to millennial time scales and show high decadal to centennial variability. This work suggests that it may be possible to incorporate some of the long term (low frequency) variability into carbon models to develop scenarios for future changes to carbon fluxes that more realistically follow long-term tree growth dynamics.

4. TREE GROWTH AND NDVI ACROSS SENSORS AND SCALES

4.1. **Background Information**

Scaling site-level processes to larger regions has been identified as a critical issue in monitoring global change [Thompson et al., 2001]. However, this remains a challenge as processes can be regulated by different factors operating across a wide range of scales. For instance, plant transpiration appears regulated by stomatal mechanisms at leaf level, though at a regional scales appears regulated by climate [Wiens, 1989]. This illustrates that the spatiotemporal scale at which an ecological phenomena is observed may be quite important and that observations at different scales may yield different patterns. Understanding the influences of landscape heterogeneity and scale of observation on the analyses of ecological processes is an area that has attracted considerable

attention in recent decades [e.g. Turner er al., 1989; Turner, 2005], in part due to the increased availability of satellite data and data processing tools (e.g. geographical information systems). Understanding the influence of scale on ecological studies is important, as studies involving remote sensing are often restricted in the spatiotemporal characteristics of data they can access and thus often end up using data with predefined spatiotemporal resolutions which may not be optimal for observing the ecological patterns of interest [Stoy et al., 2009].

Imagery from AVHRR has been archived since July 1981, thus making it a widely utilized record of land surface information [Tucker et al., 2005]. The AVHRR were originally designed for meteorological applications and thus the sensors were not optimized for vegetation monitoring as have newer sensors such as MODIS Terra and Aqua [Tucker et al., 2005]. Newer sensors permit observations at finer spatial and radiometric scales, though lack the longer data record of the older sensors and are thus limited in their use for time-series analyses. Ensuring that new sensors are compatible with the historical archive of satellite imagery requires overcoming differences in resolution—radiometric, temporal, and spatial—as well as accounting for differences in atmospheric impacts, orbital and calibration drift [Huete et al., 2002].

While NDVI has been the most widely used satellite-derived vegetation index, multiple other vegetation indices, such as the Soil Adjusted Vegetation Index [Huete, 1988] and the Enhanced Vegetation Index [EVI; Liu and Huete, 1995], have been developed in an attempt to refine satellite-based vegetation monitoring. These indices, as with NDVI, are based on absorbance at red and near-infrared wavelengths and proxy chlorophyll abundance and energy absorbance [Myneni et al., 1995]. NDVI is based on a normalized ratio which renders it largely insensitive to viewing angle and topography; however, the index shows asymptotic behavior (saturation) when used in high biomass areas and is non linear as a result of being based on a ratio [Huete et al., 2002]. The EVI has increased sensitivity in regions with high biomass, exhibits a more linear relationship with LAI, and makes use of measurements in the blue band in an effort to correct for the atmospheric effects of

ozone absorption and Rayleigh scattering [Huete et al., 2002]. Both NDVI and EVI are produced as part of the MODIS standard outputs, with NDVI being considered a "continuity index" with the AVHRR NDVI record and EVI being considered a more optimized vegetation index [Huete et al., 1999]. It is not possible to calculate EVI using AVHRR data, as AVHRR lacks a blue band with which to make the necessary atmospheric corrections. While vegetation indices other than NDVI exist, these should be viewed as complementary to the existing NDVI record.

Most studies of pan-arctic vegetation have used data from the AVHRR, while few have conducted cross-sensor or cross-scale comparisons. Interpretation of greening and browning trends from AVHRR data have been bolstered by examining the vegetation indices (VI) over a range of sensors and spatial scales, as well as by cross-sensor comparisons of the relationship among VI and measurable biophysical vegetation characteristics. Few studies at high latitudes have conducted such cross-scale and cross-sensor comparisons, thus making this an important area of research. In one of the few high-latitude cross-sensor studies, Olthof et al. [2008], stratified VI trends from Landsat and AVHRR by vegetation functional types along two regions of the Canadian taiga-tundra ecotone and found that both sensors showed similar greening of vascular and lichen vegetation communities between 1986 and 2006. Comparisons of AVHRR-derived VI with those from newer sensors, such MODIS, generally show strong agreement, though agreement can vary widely by land cover type and post-sensor processing [Gallo et al., 2005; Ji et al., 2008]. Few cross-sensor VI comparisons have been conducted in the northern high-latitudes, though Brown et al. [2006] found that these regions exhibited the highest sensor to sensor variability. In this section, tree growth was compared with NDVI from both AVHRR and MODIS across a range of grain sizes.

4.2. **Data and Methods**

4.2.1. Tree Core Sampling and Processing

See chapter three for details on tree core sampling and construction of ring-width index

chronologies. Of the 22 sites initially sampled, 14 sites from Canada and the Kolyma River were selected for use in this portion of the analysis. These sites together represented 18 tree ring chronologies. The eight Lena River sites were withheld from the analysis due to time constraints.

4.2.2. Spectral Vegetation Indices

MODIS NDVI (MOD13Q1) data were acquired from the United States Geological Survey's Land Processes Distributed Active Archive Center (lpdaac.usgs.gov), while the GIMMS NDVI were acquired from the University of Maryland's Global Land Cover Facility (GLCF; http://www.landcover.org). The MOD13Q1 product is a 250 m resolution, 16-day maximum value bi-directional surface reflectance composite. It is generated from the red (0.62-67 μm) and near infrared (0.84-0.87μ m) detectors carried aboard the NASA Terra satellites and includes atmospheric corrections [Huete et al., 1999]. The GIMMS product (Version G) is an 8 km resolution, maximum-value composite produced from channels one and two of the AVHRR sensors and includes corrections for the El Chichón and Pinatubo volcanic eruptions, as well as for solar zenith angel, sensor degradation and differences between sensors [Tucker et al., 2005]. See chapter three for a more detailed description of the GIMMS data set. MODIS has been optimized for terrestrial vegetation monitoring and is considered a successor of the AVHRR system with improved spectral, radiometric and spatial characteristics [Ji et al., 2008]. The two images for July of each year between 2000 and 2008 were acquired for each data set.

4.2.3. Satellite Image Processing

For each data set, the July images were averaged and then projected from their native formats into a North Pole Lambert Azimuthal Equal Area projection using a cubic convolution resampling technique. Water was masked from the analysis using the 250 m Global Raster Water Mask [MOD44W; Collection five; Carroll et al., 2009]. The Canadian Large Fire Database [Version two;

Stocks et al., 2002] was used to mask areas in the Northwest Territories with fires documented between 1981 and 2007. In Siberia, maps of fires occurring between 1996 and 2002 showed no documented fires in the study area [Version one; Sukhinin et al., 2004]. The fire database showed three sites in Canada as having burned during 1979 and one during 1980.

The MODIS Quality Assurance (QA) flags were checked and due to persistent cloud cover over the study period all pixels with "VI Usefulness" rating from lowest to highest were used so as to maximize the period of overlap between tree growth and satellite records. The MODIS NDVI was checked by comparing the standardized anomalies (Z-scores) of the 250 m data with Z-scores calculated from MODIS and GIMMS data spatially averaged to 24x24 km. Most sites showed close agreement in Z-scores for all three NDVI measurements; however, three sites showed low intra-MODIS correlations while showing better agreement between MODIS and GIMMS at 24 km resolutions. Time series plots of these three sites showed anomalous spikes in MODIS 250 m Z-scores which generally were not reflected in NDVI measurements at 24 km. Z-score spikes at MODIS 250 m with no corresponding change at coarser resolutions was taken as a sign of poor data quality (e.g. heavy clouds) and these sites were withheld from the analysis, leaving 14 chronologies against which NDVI was compared.

After masking and verifying the MODIS data quality, the 250 m MODIS NDVI were then spatially averaged using a moving window approach with window sizes of 3x3 (750 m), 32x32 (8 km) and 96x96 (24 km) pixels. A 3x3 pixel (24 km) averaging window was applied to the GIMMS data. A 16x16 pixel (8 km) window was also applied to the 500 m MODIS-derived Vegetation Continuous Fields tree canopy cover product [Hansen et al., 2003] to produce estimates of neighborhood tree coverage.

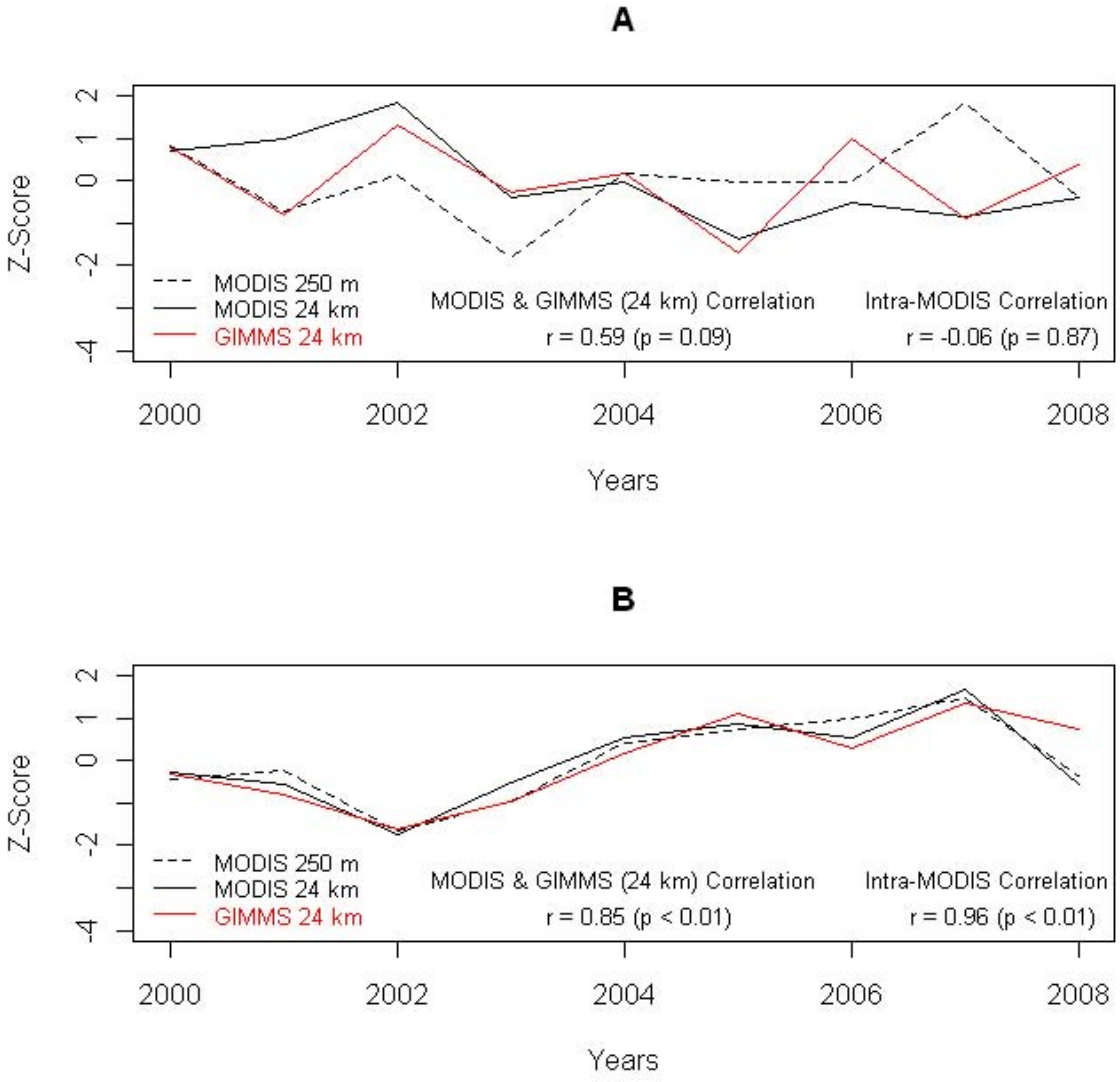

Figure 4. This figure demonstrates the method used to check for low quality MODIS data at each site. MODIS NDVI at 250 m and 24 km resolutions, as well as GIMMS at 24 km, were converted to standardized anomalies for the 2000 to 2008 period. The correlation between MODIS and GIMMS anomalies at 24 km was determined, as was the correlation between MODIS anomalies at different grain sizes. The correlation coefficients for each analysis are detailed for each site. Panel A shows a site with potentially questionable MODIS data quality, while B illustrates a site with acceptable MODIS data quality.

4.2.4. Statistical Analysis

I calculate Pearson's correlations between each RWI chronology and the corresponding six different NDVI measurements (2 x AVHRR, 4 x MODIS) over the 2000 to 2007/2008 period. *Larix* sampled during 2008 had eight years of tree growth-satellite overlap, while the *Pinus* and *Picea* sampled during 2009 had nine years. Pearson's correlation assumes data normality and this was tested using the Shapiro-Wilk test. The data from all sites except for one (SQT) were found to be normally distributed and it was not possible to transform the SQT data into a normal distribution. As was shown and corrected for in chapter one, both NDVI and RWI can exhibit autocorrelation which violates the assumptions of data independence when determining correlation significance. Autocorrelation in both NDVI and RWI was examined over the 2000 to 2008 period and none was observed, likely reflecting the short time period examined. After NDVI-RWI correlations were determined, paired Mann-Whitney U-tests were used to assess whether there were differences in correlations between MODIS grain sizes, or between MODIS and GIMMS at matching grain sizes.

4.3. **Results**

Over the 2000 to 2008 period, the correlations between NDVI and tree growth ranged from 0.17 to 0.93, with a mean ± standard deviation of 0.52 ±0.18 (Table 2; Figure 5). The number of significant correlations at a critical value of $\alpha = 0.10$ was lowest for MODIS 250 m ($n = 5$) and then increased stepwise with grain size to 24 km ($n = 8$). Both GIMMS grain sizes showed 7 significant correlations. Mann-Whitney U-tests, however, found no significant differences ($\alpha = 0.10$) between the strength of the NDVI-RWI correlations across MODIS grain sizess (Figure 5), nor between MODIS and GIMMS at matching grain sizes (Figure 6). These findings held for *Larix*, *Pinus*, and *Picea* individually, as well as across genera.

To illustrate the degree of agreement in NDVI-RWI correlations between sensors and scales, pair-wise scatter plots of correlation coefficients were created (Figure 7).The agreement between

each pair of NDVI-RWI correlation coefficients were also determined. GIMMS at both 8 km and 24 km grain sizess produced very similar correlations with tree growth ($r = 0.96$, $p < 0.001$, $df = 12$), suggesting that the landscape heterogeneity was captured equally by both grain sizes. MODIS NDVI at 250 m and 750 m resolutions yielded similar correlations with tree growth ($r = 0.77$, $p < 0.001$, $df = 12$), as did MODIS NDVI at 8 and 24 km resolutions ($r = 0.84$, $p < 0.001$, $df = 12$). Comparing the NDVI-RWI correlations produced by the two coarse resolution MODIS data sets with those of the two finer resolutions shows general agreement ($r = 0.18$ to 0.65), with the exception of a few sites. The TAL site, for example, showed NDVI-RWI correlations decreasing from $r = 0.63$ to 0.17as MODIS grain sizes increased from 250 m to 24 km, while GIMMS showed correlations of $r = 0.17$ at both grain sizes. The NDVI-RWI correlations for GIMMS and MODIS at coarse resolutions showed relatively close agreement ($r = 0.61$ to 0.84). MODIS correlations at an 8 km grain size showed equally close agreement with MODIS 24 km NDVI ($r = 0.84$, $p < 0.001$, $df = 12$), as they did those produced by GIMMS at both 8 km and 24 km resolutions ($r = 0.81$ and $r = 0.79$).

Larix showed significantly higher correlations with NDVI than did *Pinus* or *Picea* for all NDVI grain sizes except for MODIS at 250 m and 24 km (Mann-Whitney U-test, $p < 0.05$, $n = 14$). Across grain sizes average correlations with tree growth were 45% higher for *Larix* than *Picea* or *Pinus*. *Larix* also showed significantly higher interseries correlations and mean sensitivities than *Pinus* or *Picea* (Mann-Whitney U-test, $p < 0.05$, $n = 14$). Mean tree canopy cover at the *Larix* sites was 10.7% ± 2.9%, substantially lower than that of the *Picea* and *Pinus* sites (39.3 ± 7.0).

Table 2. Tree chronology metrics and correlations between tree growth and measurements of NDVI over the 2000 to 2008 period. MS = mean sensitivity, ISC = interseries correlation.

Genus	Site	Canopy Cover (%)	MODIS-RWI Correlations				GIMMS-RWI Correlations	
			250 m	750 m	8 km	24 km	8 km	24 km
Larix	DVN	6.1	0.88**	0.70*	0.75**	0.79**	0.79**	0.80**
	PAR	11.3	0.68*	0.93**	0.78**	0.67*	0.74**	0.75**
	CHE	10.7	0.53	0.60	0.74**	0.71**	0.68*	0.65*
	TRL	5.4	0.44	0.54	0.90**	0.91**	0.79**	0.81**
	ROD	11	0.60	0.66*	0.61	0.63*	0.78**	0.73**
	mean ± std	10.7 ±2.9	0.63 ±0.17	0.68 ±0.15	0.76 ±0.11	0.74 ±0.11	0.76 ±0.05	0.75 ±0.06
Picea	ELF	45.9	0.23	0.29	0.22	0.36	0.28	0.23
	SQT	37.6	0.72**	0.74**	0.53	0.32	0.70**	0.69**
	BIS	40.3	0.49	0.49	0.62*	0.49	0.53	0.51
	DAR	25.5	0.28	0.38	0.49	0.46	0.54	0.55
	TAL	38.3	0.50	0.52	0.68**	0.69**	0.56	0.57
	mean ± std	38.3 ±7.5	0.45 ±0.20	0.48 ±0.17	0.51 ±0.18	0.46 ±0.14	0.52 ±0.15	0.51 ±0.17
Pinus	ELF	45.9	0.46	0.58*	0.57	0.73**	0.46	0.27
	MKZ	42.3	0.60*	0.59*	0.71**	0.73**	0.69**	0.60*
	DAR	25.5	0.29	0.36	0.46	0.49	0.56	0.55
	TAL	38.3	0.63*	0.40	0.38	0.17	0.17	0.17
	mean ± std	40.3 ±8.9	0.49 ±0.15	0.48 ±0.12	0.53 ±0.14	0.53 ±0.26	0.47 ±0.22	0.40 ±0.21
ALL	mean ± std	25.5 ±16.2	0.52 ±0.18	0.55 ±0.17	0.60 ±0.18	0.58 ±0.21	0.59 ±0.19	0.56 ±0.21

* $p < 0.05$

** $p < 0.10$

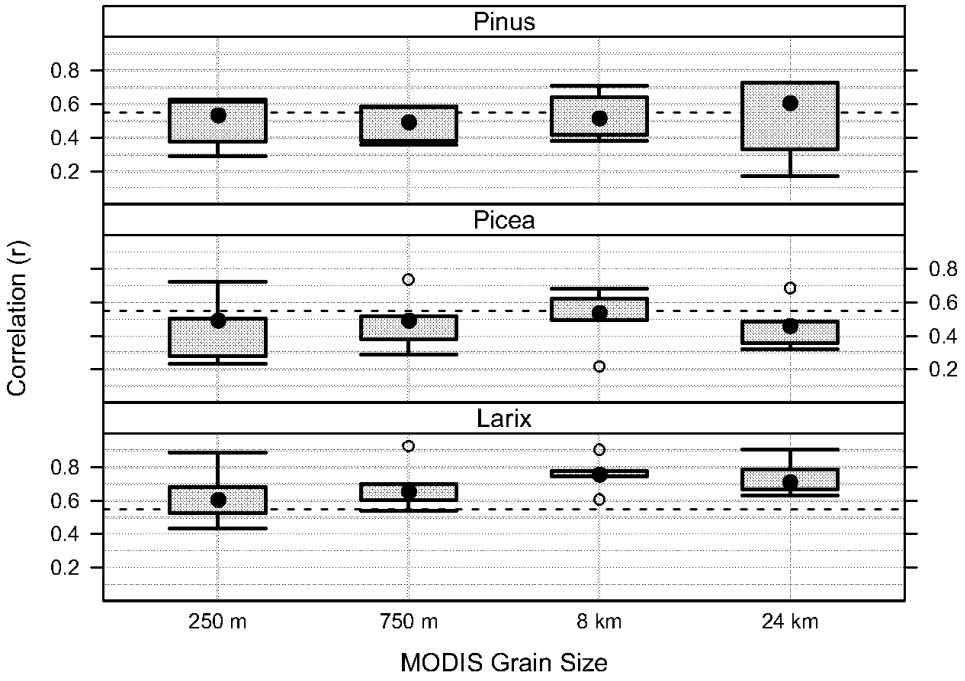

Figure 5. Correlations between tree ring indices and MODIS NDVI at four grain sizes between 2000 and 2008 for 14 sites located in western Canada and eastern Siberia. The correlations are broken down by taxa and the dashed horizontal lines indicate estimates of significance at $p = 0.05$. Intra-box dots denote medians and box edges denote the 25^{th} and 75^{th} percentiles. Whiskers represent the 5^{th} and 95^{th} percentiles, while dots denote outliers. See Table 2 for details on correlation analyses

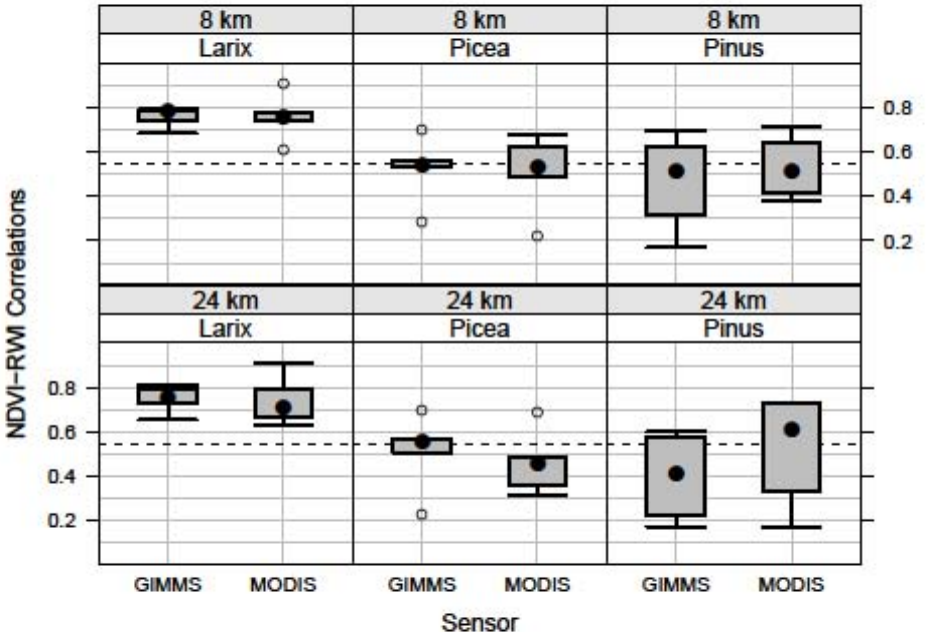

Figure 6. Box and whisker plots comparing the GIMMS and MODIS correlations with tree growth across taxa and at two grain sizes. When compared for each taxa and grain size combination, Mann-Whitney U-tests found no significant differences between GIMMS and MODIS. Intra-box dots denote medians and box edges denote the 25th and 75th percentiles. Whiskers represent the 5th and 95th percentiles, while dots denote outliers.

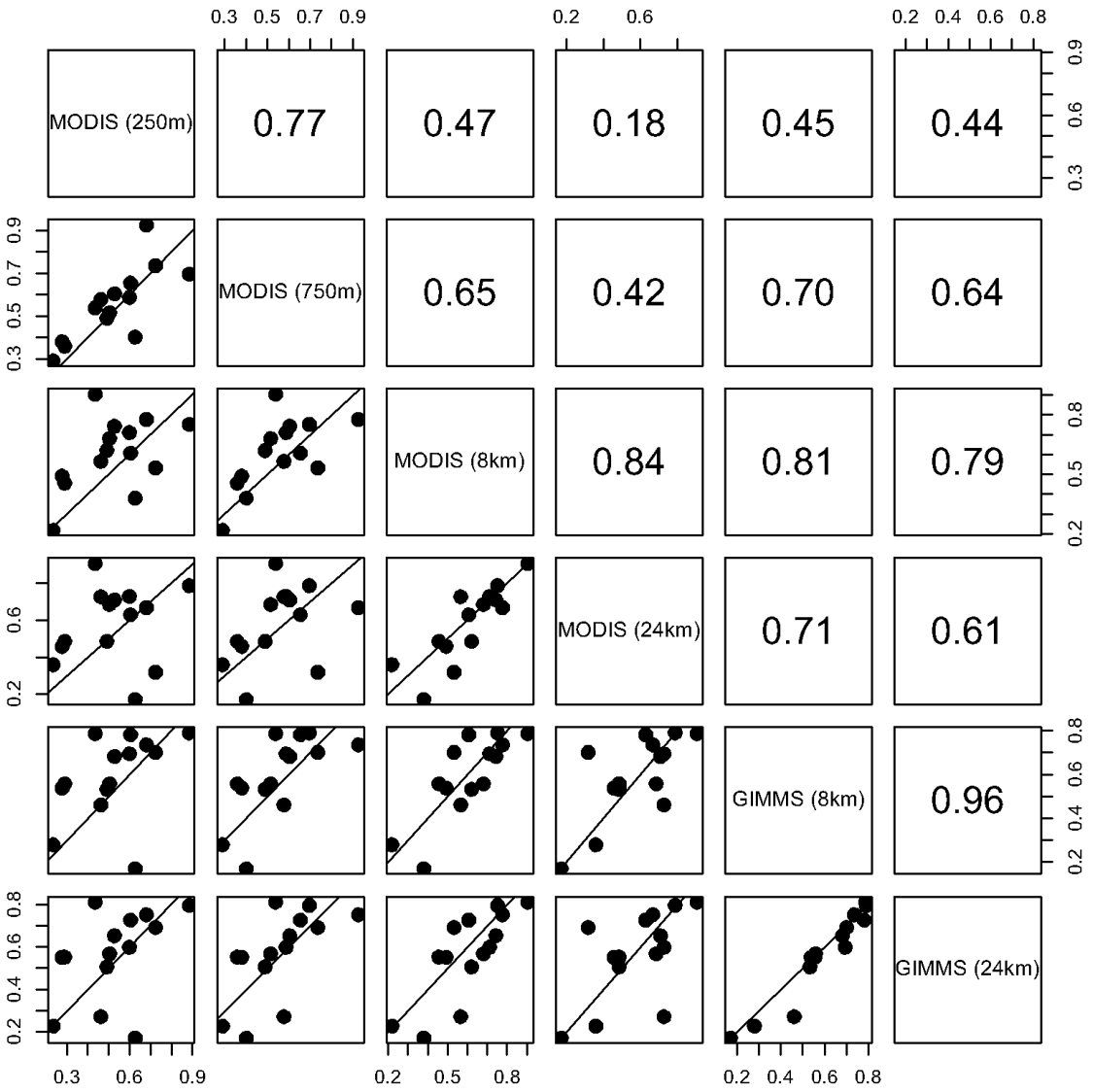

Figure 7. Pair-wise scatter plots comparing the strength of the NDVI-RWI correlations across the six measurements of NDVI. Each point represents a sampling site. The upper off-diagonal shows the correlations for each comparison. Correlations with $r > 0.43$ are significant at $p = 0.05$ and $n = 14$. Within each plot, the diagonal line represents a 1:1 relationship. Note that GIMMS and MODIS exhibit similar correlations with RWI across both 8 km and 24 km grain sizes. Additionally, intra-MODIS comparisons show good agreement between RWI correlations at the two finer resolutions, as well as between the two coarser resolutions.

4.4. **Discussion**

The relationship between tree-ring indices and space-borne measurements of NDVI has received attention over the past decade as a means of increasing the spatial extent of tree growth measurements. Studies have documented significant relationships between tree-ring indices and NDVI during summer months in areas throughout the northern hemisphere using AVHRR data [Kaufmann et al., 2004, 2008; Wang et al., 2004; Lopatin et al., 2006]. Our results, while based on a limited number of sites (n = 11), years (n = 9), tree genera (n = 3), and post-sensor processing methods, suggest that MODIS and AVHRR at similar resolutions can proxy tree cambial growth to very similar extents in some regions. The GIMMS data set is processed in such a way as to make the AVHRR data compatible with the dynamic range of SPOT Vegetation and MODIS sensors [Tucker et al., 2005]. In spite of differences in sensor bandpasses, compositing techniques, atmospheric corrections, equatorial cross times, and data resampling [Ji et al., 2008], these findings demonstrate strong similarities between sensors in a region where large discrepancies in these vegetation indices have previously been observed [Brown et al., 2006].

The agreement between sensors is significant for a number of reasons. As previously noted, few applied cross-sensor comparisons of vegetation indices have been conducted at high-latitudes. The agreement between sensors helps to bolster confidence in both the utility of the historical AVHRR record and in the observed relationship between tree growth and NDVI. The finding also suggests that it might be possible to bridge together MODIS and AVHRR data sets to capitalize on the higher radiometric and spatial resolutions of MODIS and the more frequent overpasses by made AVHRR. Past work has demonstrated that VI can generally be interconverted with a precision of 1-2% [Steven et al., 2003], which is important given the frequency of cloud cover, changes in technology, and satellite longevity.

Assuming adequate spatial precision in satellite and tree stand coordinates, I hypothesized that NDVI measured at finer spatial scales would correlate more strongly with tree growth than

coarser resolution measurements. My results, however, did not support this hypothesis and instead showed relatively consistent correlations across four gain sizes from 250 m to 24 km. The lack of observed spatial dependence may partially reflect how the satellite data were processed, as well as similarities in inter-annual NDVI variability between some forest and non-tree vegetation. We masked both water bodies and burned areas, two land cover types that frequently occur in boreal and sub-arctic ecosystems and that possess very different NDVI signals from surrounding vegetation [Hope et al., 2004; Goetz et al., 2006]. Masking such land cover types thus reduces the non-vegetation related variability in NDVI that is encountered as grain size increases.

In discussing vegetation-related changes in NDVI associated with increasing grain sizes, it should first be noted that most of the sites were open-canopy stands with VCF estimates of tree canopy cover ranging from 5% to 46% (mean ± sd = 31.6 ± 15.6; Table 1). The radiometric contribution of understory vegetation—shrubs, herbs, mosses, lichens—to the signal recorded by the satellites makes it difficult to isolate the signal associated with a particular functional group (e.g. trees) [Goetz and Prince, 1996]. The VCF product, for instance, tends to overestimate tree canopy cover in sparsely forested areas due to inclusion of shrubs, which can possess similar radiometric characteristics [Montesana et al., 2009]. While the NDVI signal may reflect non-tree vegetation as well, D'Arrigo et al. [2000] suggest that if a tree ring parameter and regional productivity are limited by the same environmental influences then tree ring measurements from an individual species covering a small proportion of the landscape may serve as an approximate index of regional production. While it is possible that increasing grain size may lead to inclusion of a broader array of vegetation types, or changes in the proportion of vegetation types, the vegetation may exhibit a degree of synchronicity in both growth (e.g. foliage production) and growth-related NDVI if regulated by similar environmental constraints.

Contrasting the Siberian (n = 5) and Canadian (n = 6) sites supports the idea that when a similar factor is limiting both tree productivity and more ecosystem-wide productivity, then tree

rings may serve as an approximate index of regional growth. In spite of canopy cover at the *Larix* sites in eastern Siberia being approximately 42% that of the Canadian sites, *Larix* showed significantly higher NDVI-RWI correlations over the 2000 to 2008 period across nearly all measurements of NDVI than did the *Pinus* or *Picea* sites in Canada . Annual NDVI over the eastern Siberian taiga-tundra correlates very strongly with a warmth index [r = 0.92; Suzuki et al., 2000], while other work also supports the view that vegetation production in the region is primarily temperature-limited, directly or indirectly [Nemani et al., 2003; Bunn et al., 2007]. Nearly 8° further south, our Canadian boreal forest sites broadly show a mixture of temperature and water-induced constraints [Nemani et al., 2003; Bunn et al., 2007]. Additionally, the Siberian study area is underlain by continuous permafrost, while the Canadian area is underlain by discontinuous permafrost [Brown et al., 1997]. Larger potential variations in permafrost depth at the Canadian sites may also have led to a wider range of growth behaviors across the landscape. The combination of abiotic limitations and higher tree diversity at the Canadian sites than at the Siberian sites means that vegetation phenology and growth may vary more widely across the landscape and thus tree ring measurements from a single species covering a small area may not serves as a robust proxy of regional growth. Under conditions where vegetation growth is highly variable across the landscape, NDVI and tree ring measurements will show lower agreement because NDVI will represent a radiometric blend of vegetation types. This may help explain the significantly lower NDVI-RWI correlations between 2000 and 2008 at the Canadian sites, as well as the lack of observed spatial dependence in NDVI-RWI correlations.

The almost exclusive use of AVHRR in monitoring global high-latitude vegetation dynamics [e.g. Angert et al., 2005; Bunn et al., 2007; Zhang et al., 2008] illustrates how data limitations can set constraints on scales of observation, as the use of AVHRR largely derives from its relatively long data record and less so from the particular spatiotemporal resolutions of the sensors. While the legacy of U.S. satellite missions may guide ecological researchers towards using AVHRR,

cross-sensor and scale comparisons have demonstrated the continued utility of the historical AVHRR data archive. Olthof et al. [2008], for example, assessed vegetation-specific NDVI trends over two regions of the Canadian tree line and found that one kilometer AVHRR and 30 m Landsat measurements yielded similar trends over recent decades. Hope et al. [2004] compared spatially-averaged AVHRR NDVI with that from a moderate resolution air-borne sensor along the north coast of Alaska and found that while the AVHRR values were consistently lower and exhibited less variability, these differences were systematic and the sensors showed the same general patterns in NDVI. The researchers noted that the aircraft measurements exhibited higher variability likely owing to the extensive presence of small lakes which depressed the aircraft measurements to a greater extent than the AVHRR NDVI, which necessarily blended surrounding vegetation with the lakes owing to the larger pixel size. In this study, NDVI from both AVHRR and MODIS was examined in relation to tree growth across a range of scales and land cover types, demonstrating that the two sensors showed general agreement at many sites across scales of observation encompassing two orders of magnitude.

The purpose of this work was to help improve our ability to interpret trends in NDVI over high-latitude forested regions through the use of cross-platform and cross-scale comparisons so as to gain a better understanding of forest productivity in these regions. To this end I have shown that MODIS and GIMMS yielded similar correlations with tree growth at select sites, as did measurements of NDVI across multiple MODIS grain sizes. Additionally, the results indirectly support the hypothesis of D'Arrigo et al. [2000] that a tree ring parameter can serve as an index of regional productivity in regions where both tree growth and NPP are limited by the same environmental factors. Our study is limited by the short period of overlap between measurements of tree growth and MODIS NDVI (n = 8 or 9 years), the modest number of sampling sites (n = 11), and by conducting the comparison only during the month of July. Additional work should examine the influence of landcover composition on the agreement between sensors and scales, as well as the

growth and NDVI response of vegetation to climate.

5. SUMMARY and CONCLUSIONS

5.1. **Summary**

This study demonstrated the utility of two space-borne sensors of widely different spatial and radiometric characteristics to proxy forest growth at some high latitude locations. The relationship between NDVI and tree ring indices was highly variable over the 1982 to 2008 period, though displayed consistent positive associations across *Picea*, *Pinus*, and *Larix* genera. Over this period, marked differences between evergreen and deciduous conifers were observed in both the NDVI and RWI autocorrelation structures. *Larix*, a deciduous conifer, showed no year to year persistence in canopy development, as proxied by NDVI, while *Picea* and *Pinus*, both evergreen conifers, displayed multi-year persistence. The annual radial growth increment measurements showed autocorrelation patterns similar to those of the NDVI, with higher inter-annual variability in *Larix* and lower inter-annual variability in evergreens. Evergreen conifers can use stored photosynthates to buffer canopy and radial growth during difficult years, whereas deciduous conifers must use a greater proportion of stored energy to rebuild leaf area, thereby reducing energy available to buffer growth. Autocorrelation within NDVI measurements has not been widely investigate in the literature, particularly in terms of contrasting patterns between functionally-distinct tree genera. While NDVI and RWI showed consistent positive associations over the 28 year period, the low to moderate correlations between NDVI and RWI suggest that ring-width is controlled by a variety of factors, potentially spanning many years, and not just by rates of photosynthesis or canopy development [Rocha et al., 2006].

In addition to examining the GIMMS NDVI-RWI correlations over the 1982 to 2008 period, MODIS and GIMMS were examined over a 9 year period across scales of observation.
This analysis showed that MODIS and GIMMS produced similar correlations with ring-width

indices across most of the sampling sites. Differences in correlations may reflect the combined effect of differences in sensor bandpasses, resampling, and post-sensor corrections for orbital drift, sensor decay, and atmospheric influences. Cross-sensor studies are important as a mean of verifying observations from one sensor and suggest that finer resolution data with shorter record lengths can be used, in some cases, to augment longer data records from sensors that may have poorer spatial or radiometric resolutions.

MODIS and AVHRR NDVI produced similar correlations with ring-width indices, as did MODIS NDVI over four grain sizes ranging from 250 m to 24 km. The lack of observed spatial dependence in NDVI-RWI correlations after masking water and burned regions from the analysis area supports the hypothesis of D'Arrigo et al. [2000] that tree ring width indices may serve as an approximate indicator of regional productivity in places where tree growth and regional production are limited by the same factors. The low to moderate forest cover at the sampling sites means that understory vegetation contributed heavily to the radiometric signal recorded by the satellites at all scales of observation. Thus, while increasing grain size may potentially lead to changes in vegetation composition, the vegetation may show a degree of inter-annual synchronicity in productivity.

5.2. **Limitations and Uncertainty**

In this study estimates of tree growth were related to space-borne observations of photosynthetic activity at 22 sites concentrated in western Canada and central to eastern Russia. Specifically, an effort was made to characterize stand-level forest growth using tree ring measurements and then to relate interannual variations in growth to a remotely-sensed metric that correlates strongly with leaf area index (LAI) and absorbed photosynthetically-active radiation. The purpose of this work was to evaluate the relationship between NDVI and tree growth so as to help ground truth NDVI-based model results suggesting decreased forest productivity in many boreal forest regions.

Comparisons between tree growth and satellite-derived vegetation indices are complicated by a number of factors, most of which are related to the differences in the scale at which each technique senses growth. A number of potential sources of error and limitations arise and these can generally be related to characterization of growth using tree rings, satellite sensors and processing, and biological plasticity.

Limited samples and multi-species stands are two of the factors that complicated capturing common growth signals across large areas using tree ring measurements. Using measurements from a limited number of trees to describe forest-level growth patterns is one potential source of error in this study. Samples were taken from a limited number of conifers over a small geographic area—generally a few hectare—and then related to satellite data covering areas ranging from 6.25 ha to 57,600 ha. Tree growth can vary significantly among individual trees within a small area as a result of microhabitat variability, small-scale disturbances (e.g. insects or blowdown) and species-specific differences. While sampling sites may have appeared roughly representative of the surrounding area, significant variation in composition and growth may have occurred within the satellite footprint and not have been captured by the trees sampled. Another limitation involved how canopy co-dominant stands were handled. Where co-dominance occurred between conifers, separate chronologies were created for each taxa and NDVI was compared with each. Deciduous species, such as birch (*Betula spp.*), occurred at some sites, principally in Canada, though were not sampled and thus their growth patterns were not represented in our chronologies.

Vegetation indices represent a blend of canopy and understory vegetation. Tree canopy cover at the sampling sites ranged from an estimate 9% to 53% (mean = 32% ± 14%) with large amounts of shrub and herbaceous plant cover. The variability in tree cover means that background vegetation contributed to varying extents to the NDVI measurement. Kobayashi et al. [2007], for example, studied the spectral development of a *Larix* forest through the growing season near Yakutsk, Russia, close to where samples from this study were collected, and found that understory green-up led to

NDVI achieving 71% of the season's maximum prior to canopy foliation. Other researchers have previously noted the pronounced radiometric effect of understory vegetation in sparsely forested areas, such as along the tundra-taiga boundary [Goetz and Prince, 1996; Rees et al., 2002]. Imagery that incorporates mixed species stands into individual pixels will represent some blend of potentially contrasting growth patterns; potentially obscuring relations that might otherwise be apparent in single species stands [Lopatin et al., 2006]. Determining a means by which to partition the NDVI signal between different land cover types in a mixed pixel would be a timely and beneficial avenue of research.

Another potential source of uncertainty in this study involves having used data from multiple sensors spanning nearly ten to thirty years of operation. In this study, data from two MODIS sensors and 6 AVHRR sensors were used, with MODIS and AVHRR-derived GIMMS undergoing different processing methods. Processing for both sensors includes the use a maximum-value compositing technique; however, the techniques differ. While GIMMS uses a straight maximum-value composite (MVC), MODIS employs a constrained angle, maximum value bidirectional reflectance technique [Gallo et al., 2004]. Processing further differs in that the MODIS product includes a correction for atmospheric water vapor and aerosols, where as GIMMS does not. The MVC technique reduces the influence of factors that would artificially depress NDVI, such as forest fire emissions or water vapor; however, GIMMS does not directly correct for these potential sources of error [Tucker et al., 2005].

In processing the remote sensing data an effort was made to exclude from the analysis areas of water and recent fire activity. Water was excluded using the Global Raster Water Mask based off of 250 m resolution MODIS data [Carroll et al., 2009]. Small bodies of water or water with vegetation cover (e.g. bogs) might not have been captured by the mask and thus would have depressed the NDVI signal for those pixels. While an effort was also made to exclude fires from the analysis areas, limited data were available. Only seven years of burn data (1996-2002) were

available for Russia. In Canada fires > 2 km^2, representing an estimated 97% of the total burned area were masked between 1981 and 2007 [Stocks et al., 2002].Vegetation recovering from fires before or after these periods may have different climate responses than unburned vegetation, thus generating different NDVI values. No additional disturbance data (e.g. insect or logging) were included in this analysis.

Another potential source of uncertainty in relating tree ring indices with NDVI involves the dynamic allotment of nutrients between different organs depending on environmental constraints. Changes in water and temperature regimes may shift the allometric relations between production of roots, shoots, and radial growth [Larcher, 1995]. Lapenis et al. [2005] examined repeated forest inventory data at 3196 sample plots throughout Russia and found evidence that since the 1950s the ratio of shoot to root production had changed. In European Russia, higher summer temperatures and precipitation have accompanied increased leaf and needle production, while in the northern taiga warmer and drier conditions have occurred concurrent with reductions in leaf area and increased root production.

5.3. **Future Work**

There are a number of additional steps that could be taken to build upon this work. This study has demonstrated that NDVI can proxy high-latitude tree growth under some circumstances, that autocorrelation in NDVI occurs within evergreen though not deciduous conifer stands, and that MODIS and AVHRR yield similar correlations with RWI across multiple grain sizes. Additional work could attempt to refine and further investigate these conclusions. Broadly, additional work could focus on different techniques for developing tree ring chronologies, modeling tree growth using NDVI, and understanding the influence of land cover and scale of observation on NDVI. The following are some potential avenues of inquiry:

1. The tree ring chronologies used in this study represented individual species even for stands in which canopy cover exhibited species co-dominance. Chronologies from individual taxa could be weighted and bridged in order to create a single chronology more representative of stand-level forest dynamics. The proportion of canopy cover for each species could be used as the weighting factor. Developing mixed-species chronologies represents probably one of the more important follow ups to this study, as single species chronologies may not capture landscape-level growth in areas where growth patterns vary widely.

2. Trends in NDVI and RWI should be directly examined in relation to inter-annual climate variability. Finding evidence of differences in NDVI and RWI autocorrelation between deciduous and evergreen conifers implies that lagged effects need to be taken into consideration when when modeling growth-NDVI-climate responses. Preliminary work using our data suggests that the relationship between NDVI and RWI may change over time; however, the short data record did not permit a robust analysis (Appendix 3).

3. The growing season definition for selection of NDVI periods against which to compare tree growth could be investigated further. In this study mean July NDVI was used, as well as a growing season mean based off of the latest green-up and earlier brown-down dates occurring between 2000 and 2004. One avenue might involve using gridded climate data tied with NDVI to model site variation in growing season length. The shorter time but higher resolution MODIS record could be used to examine green-up and brown-down periods as functions of weather data and then use the historical weather data to backcast site-level growing season lengths. This would permit the growing season to change in length instead of remaining invariant between years and would help to capture potential changes in tree growth associated with changes in the length of the growing season.

4. Instead of comparing tree ring indices directly with NDVI, they could instead be related to PEM-derived estimates of NPP. The VCF data could be tied with the PEM and used to model NPP along the large tree-herb gradient. This would help to place NDVI in a more biologically-meaningful context.

5. The influence of land cover on the agreement between MODIS and GIMMS NDVI should be examined. This might help to clarify situations under which differences in correlations with tree growth occur. One approach would be to examine how the correlation between sensors changes as a function of land cover. See Appendix 4 for a preliminary example. Additionally, the vegetation continuous field (VCF) products could be used to extract NDVI signals within each sampling window for areas with moderate to high levels of tree cover, thus excluding pixels with barren earth and herb-dominated radiometric signals. The VCF products could also be used to weight NDVI by the proportion of each pixel occupied by tree cover, again trying to isolate the radiometric signal produced by forest cover and exclude that of background land cover.

6. Spatial scaling of NDVI over a wider range of grain sizes might produce a better understanding of how land cover and vegetation heterogeneity influence the correlation between NDVI and tree growth. This could be done using MODIS or a higher resolution sensor such as Landsat. One avenue might involve scaling MODIS step-wise from 250 m (1x1 pixel) to 24 km (96x96 pixels) and then correlating each step with tree growth. Scaling the VCF products over the same range might then permit the influence of land cover to be further determined.

7. Additional work should look for potential saturation of the NDVI signal over high biomass areas and investigate how this might impact NDVI-RWI correlations. The NDVI correlations could be compared with those generated using the Enhanced Vegetation Index, which includes a blue-band correction for atmospheric disturbances and does not saturate as easily. Also, a practical means of working with the MODIS QA data need to be found. The inability to selectively mask out data of poor quality may have been a potential source of error even after excluding four chronologies from the analysis where data quality was questionable.

5.4. **Conclusions**

The northern high-latitudes have experienced more rapid rates of climate change than most areas at lower latitudes. Model projections suggest that by the end of the 21st century, mean annual temperatures above 60° N will be 4° to 7° C warmer than present, with precipitation potentially increasing 20% [ACIA, 2004]. Numerous lines of evidence point towards an array of recent changes in the physical and ecological conditions at high-latitudes. Earlier snow free periods, declining glacier and sea ice extent, increased permafrost and surface temperatures, as well as changes in the range and behavior of plants and animals have all been documented in recent years [Hinzman et al. 2005]. Changes in vegetation and land cover resulting from climatic perturbations or change in disturbance regimes can induce climate feedbacks with potentially adverse consequences [Chapin et al., 2005]. Understanding the magnitude, rate and spatial extent of changes is of great importance for quantifying climate-carbon feedbacks, though is a tremendous challenge, as North American and Eurasian land masses above 50° N cover ~25 million km^2 and are both sparsely populated and instrumented.

Remote sensing thus has an important role to play in linking studies conducted at fine spatial scales with regional to continental scale phenomena. Linking ground-based biophysico measurements to space-borne measurements it is possible to extend the potential range of inferences

which may be drawn and thus provide a more complete picture of Arctic and boreal changes. In doing so it is important that efforts be made to compare satellite observations across sensors and spatial scales so as to account for potential difference between sensors, as well as to determine proper resolutions at which phenomena should be observed. This work demonstrates one application linking space-borne measurements of photosynthetic activity with field-based measurement of forest growth and in doing so highlights some of the limitations and future potentials of using remote sensing approaches to monitor changes in high latitude ecosystems dynamic.

REFERENCES

Angert, A., S. Biraud, C. Bonfils, C.C. Henning, W. Buermann, J. Pinzon, C.J. Tucker, and I. Fung (2005), Drier summers cancel out the CO2 uptake enhancement induced by warmer springs, *Proc. Natl. Acad. Sci., 102*, 10823-10827.

Arctic Climate Impact Assessment (2004), *Impacts of a Warming Arctic - Arctic Climate Impact Assessment*, 146 pp., Cambridge Univ. Press, Cambridge, U.K.

Barber, V., G. P. Juday, and B. Finney (2000), Reduced Growth of Alaskan White Spruce in the Twentieth Century from Temperature-Induced Drought Stress, *Nature, 405*, 668–673.

Bascietto, M., P. Cherubini, and G. Scarascia-Mugnozza (2004), Tree rings from a European beech forest chronosequence are useful for detecting growth trends and carbon sequestration, *Can. J. For. Res.,34,* 481-492.

Beck, P.S.A., P. Jonsson, K.A. Hogda, S.R. Karlsen, L. Eklundh, and A.K. Skidmore (2007), A ground-validated NDVI dataset for monitoring vegetation dynamics and mapping phenology in Fennoscandia and the Kola peninsula, *Int. J. Rem. Sens., 28*, 4311-4330.

Berexovskaya, S., D. Yang and D.L. Kane (2004), Compatibility analysis of precipitation and runoff trends over the large Siberian watersheds, *Geophys. Res. Lett., 31*, L21502, doi:10.1029/2004GL021277.

Biondi, F. (1999), Comparing tree-ring chronologies and repeated timber inventories as forest monitoring tools, *Ecol. Appl., 9*, 216-227.

Bouriaud, O., N. Breda, J.-L. Dupouey, and A. Granier (2005), Is ring width a reliable proxy for stem-biomass increment? A case study in European Beech, *Can. J. For. Res., 35*, 2920-2933.

Brown, J., Ferrians, O.J.J., Heginbottom, J.A. and Melnikov, E.S. (1997), International Permafrost Association Circum-Arctic Map of Permafrost and Ground Ice Conditions, Scale 1:10,000,000, U.S. Geological Survey.

Brown, M.E., J.E. Pinzon, K. Didan, J.T. Morisette, and C.J. Tucker (2006), Evaluation of the consistency of long-term NDVI time series derived from AVHRR, SPOT-Vegetation, SeaWiFS, MODIS, and LandSAT ETM + Sensors, *IEEE Transact. Geosci. Rem. Sens.*, doi: 10.1109/TGRS.2005.860205.

Bunn, A. G., and S. J. Goetz (2006), Trends in circumpolar satellite observed gross photosynthesis from 1982–2003: The role of cover type and vegetation density, *Earth Interact., 10*, 1–19.

Bunn, A.G., S.J. Goetz, J.S. Kimball, and K. Zhang (2007), Northern high-latitude ecosystems respond to climate change, *Eos, 88,* 333-340.

Bunn, A.G. (2008), A dendrochronology program library in R (dplR), *Dendrochronologia, 26,* 115-124.

Bunn, A.G. (In press), Statistical and visual crossdating in R using the dplR library, *Dendrochronologia*.

Burn C.R. and S.V. Kokelj (2009), The Environment and Permafrost of the Mackenzie Delta Area, *Permafrost Periglacial Processes, 20,* 83-105.

Carroll, M., J. Townshend, C. DiMiceli, P. Noojipady, R. Sohlberg (2009), A New Global Raster Water Mask at 250 Meter Resolution. *Int. J. Digital Earth,* (in press).

Chapin III, F.S., A.D. McGuire, J. Randerson, R. Pielker Sr., D. Baldocchi, S.E. Hobbie, N. Roulet, W. Eugster, E. Kasischke, E.B. Rastetter, S.A. Zimov, and S.W. Running (2000), Arctic and boreal ecosystems of western North America as components of the climate system, *Global Change Biol., 6,* 211-223.

Chapin III, F.S., M. Strum, M.C. Serreze, J.P. McFadden, J.R. Key, A.H. Lloyd, A.D. McGuire, T.S. Rupp, A.H. Lynch, J.P. Schimel, J. Beringer, W.L. Chapman, H.E. Epstein, E.S. Euskirchen, L.D. Hinzman, G. Jia, C.-L. Ping, K.D. Tape, C.D.C. Thompson, D.A. Walkter, and J.M. Welker (2005),

Role of Land-Surface Changes in Arctic Summer Warming, *Science, 310*, 657-660, doi:10.1126/science.1117368.

Cramer, W., D. Kicklighter, A. Bondeau, B. Moore III, G. Churkina, B. Nemry, A. Ruimy, A. Schloss, and the participants of the Potsdam NPP Model Intercomparision (1999), Comparing global models of terrestrial net primary productivity (NPP): overview and key results, *Global Change Biol., 5*, 1-15.

D'Arrigo, R.D., Jacoby, G.C., and Fung I.Y. (1987), Boreal forests and atmosphere-biosphere exchange of carbon dioxide, Nature, 329, 321-323.

D'Arrigo, R.D., C.M. Malmstrom, G.C. Jacoby, S.O. Los, and D.E. Bunker (2000), Correlation between maximum latewood density of annual tree rings and NDVI based estimates of forest productivity, *Int. J. Remote Sens., 21*, 2329-2336.

Dawdy, D.R., and N.C. Matalas (1964), Statistical and probability analysis of hydrological data, part III: Analysis of variance, covariance and time series, in *Handbook of Applied Hydrology, a Compendium of Water-Resources Technology*, edited by V.T. Chow, pp. 8.68-8.90, McGraw-Hill, New York., U.S.A.

Devi N., F. Hagedorn, P. Moiseev, H. Bugmann, S. Shiyatov, V. Mazepa, and A. Rigling (2008), Expanding forests and changing growth forms of Siberian larch at the Polar Urals treeline during the 20th century, *Global Change Biol., 14*, 1581-1591, doi: 10.1111/j.1365-2486.2008.01583.x.

Ecological Stratification Working Group Agriculture and Agri-Food Canada, Research Branch, Centre for Land and Biological Resources Research and Environment Canada, State of the Environment Directorate, Ecozone Analysis Branch (1995), A National Ecological Framework for Canada., Ottawa/Hull, Report and national map at 1:7500 000 scale.

Esper, J., D. Frank, U. Buntgen, A. Verstege, R.M. Hantemirov, and A.V. Kirdyanov (2009), Trends and uncertainty in Siberian indicators of 20th century warming, *Global Change Biol.,* doi: 10.1111/j.1365-2486.2009.01913.x

European Commission Joint Research Center (2003), Global Land Cover 2000 database, <http://bioval.jrc.ec.europa.eu/products/glc2000/glc2000.php>.

Fritts, H.C. (2001), *Tree Rings and Climate*, Blackburn Press, Caldwell, U.S.A.

Gallo, K., L. Ji, B. Reed, J. Eidenshink, and J. Dwyer (2005), Muli-platform comparisons of MODIS and AVHRR normalized difference vegetation index data, *Remote Sens. Environ., 99*, 221-231.

Goetz, S.J. and S.D. Prince (1996), Remote sensing of net primary production in boreal forest stands, *Agric. For. Meteorol., 78*, 149-179. doi:10.1016/0168-1923(95)02268-6.

Goetz, S. J., A. Bunn, G. Fiske, and R. A. Houghton (2005), Satellite observed photosynthetic trends across boreal North America associated with climate and fire disturbance, *Proc. Natl. Acad. Sci.,102*, 13,521–13,525.

Goetz, S.J., G.J. Fiske, and A.G. Bunn (2006), Using satellite time-series data sets to analyze fire disturbance and forest recovery across Canada, *Remote. Sens. Environ., 101,* 352-365. doi:10.1016/j.rse.2006.01.011.

Gower, S.T., and J.H. Richards (1990), Larches: Deciduous Conifers in an Evergreen World, *BioScience, 40,* 818-826.

Gower, S.T., P.B. Reich, Y. Son (1993), Canopy dynamics and aboveground production of 5 tree species with different leaf longevities, *Tree Physiol., 12,* 327-345.

Gower, S.T., O. Krankina, R.J. Olson, M. Apps, S. Linder, and C. Wang (2001), Net primary production and carbon allocation patterns of boreal forest ecosystems, *Ecol. Appl., 11*, 1395-1411.

Graumlich, L.J., Brubaker, L.B., and Grier, C.C. (1989), Long-term trends in forest net primary productivity: Cascade Mountains, Washington, *Ecology, 70,* 405-510.

Hansen, M., R.S. DeFries, J.R.G. Townshend, M. Carroll, C. Dimiceli, and R.A. Sohlberg (2003), Global Percent Tree Cover at a Spatial Resolution of 500 Meters: First Results of the MODIS Vegetation Continuous Fields Algorithm, *Earth Interact.,7*, 1-15, doi: 10.1175/1087-3562.

Hinzman, L.D., N.D. Bettez, W.R. Bolton, F.S. Chapin, M.B. Dyurgerov, C.L. Fastie, B. Griffith, R.D. Hollister, A. Hope, H.P. Huntington, A.M. Jensen, G.J. Jia, T. Jorgenson, D.L. Kane, D.r. Klein, G. Korinas, A.H. Lynch, A.H. Lloyd, A.D. McGuire, F.E. Nelson, W.C. Oechel, T.E. osterkamp, C.H. Racine, V.E. Romanovsky, R.S. Strone, D.A. Stow, M. Sturm, C.E. Tweedie, G.L. Vourlitis, M.D. Walker, D.A. Walker, P.J. Webber, J.M. Welker, K.S. Winker, and K. Yoshikawa

(2005), Evidence and implications of recent climate change in northern Alaska and other Arctic regions, *Climatic Change, 72*, 251-298.

Holmes, R.L. (1983), Computer-assisted quality control in tree-ring dating and measurement, *Tree-Ring Bulletin, 43*, 69-78.

Hope, A.S., K.R. Pence, and D.A. Stow (2004), NDVI from low altitude aircraft and composited NOAA AVHRR data for scaling Arctic ecosystem fluxes, *Int. J. Rem. Sens., 25*, 4237-4250.

Hudson, J. M. G., and G. H. R. Henry (2009), Increased plant biomass in a High Arctic heath community from 1981 to 2008, *Ecology, 90*, 2657-2663.

Huete, A.R. (1988), A soil adjusted vegetation index, *Rem. Sens. Environ., 25*, 295-309.

Huete, A., C. Justice, and W. van Leeuwun, (1999), MODIS Vegetation Index (MOD13) Algorithm Theoretical Basis Document, Version 3, Tuscon, University of Arizona. <http://modis.gsfc.nasa.gov/data/atbd/atbd_mod13.pdf>.

Huete, A., K. Didan, T. Miura, E.P. Rodriguez, X. Gao, and L.G. Ferreira (2002), Overview of the radiometric and biophysical performance of the MODIS vegetation indices, *Rem. Sens. Environ., 83*, 195-213.

Intergovernmental Panel on Climate Change (2007), Contribution of Working Group I to the Fourth Assessment Report of the Intergovernmental Panel on Climate Change, edited by S. Solomon, D.

Qin, M. Manning, Z. Chen, M. Marquis, K.B. Averyt, M. Tignor and H.L. Miller, Cambridge Univ. Press, Cambridge, U.K.

Jia, G. J. E., E. Howard, D.A. Walker (2003), Greening of arctic Alaska, 1981-2001. *Geophys. Res. Lett., 30*, 2067, doi:2010.1029/2003GL018268.

Ji, L., K. Gallo, J.C. Eidenshink, and J. Dwyer (2008), Agreement evaluation of AVHRR and MODIS 16-day composite NDVI data sets, *Int. J. Rem. Sens., 29*, 4839-4861.

Kaufmann, R.K., R.D. D'Arrigo, C. Laskowski, R.B. Myneni, L. Zhou, and N.K. Davi (2004), The effect of growing season and summer greenness on northern forests, *Geophys. Res. Lett., 31*, L09205, doi:10.1029/2004GL019608.

Kaufmann, R.K., R.D. D'Arrigo, L.F. Paletta, H.Q. Tian, W.M. Jolly, and R.B. Myneni (2008), Identifying Climatic Controls on Ring Width: The Timing of Correlations between Tree Rings and NDVI, *Earth Interact., 12*, 14, doi: 10.1175/2008EI263.1.

Kaufman, D.S., D.P. Schneider, N.P. Mckay, C.M. Ammann, R.S. Bradley, K.R. Briffa, G.H. Miller, B.L. Otto-Bliesner, J.T. Overpeck, B.M. Vinther, and Arctic Lakes 2k Project Members (2009), Recent warming reverses long-term Arctic cooling, *Science, 325*, 1236-1239.

Kimball, J.S., M. Zhao, K.C. McDonald, and S.W. Running (2006) Satellite remote sensing of terrestrial
net primary production for the pan-Arctic basin and Alaska, *Mitigat. Adapt. Strategies Global Change*,

11, 738-804, doi: 10.1007/s11027-005-9014-5.

Kobayashi, H., S. Suzuki, and S. Kobayashi (2006), Reflectance seasonality and its relation to the canopy leaf area index in an eastern Siberian larch forest: Multi-satellite data and radiative transfer analysis, *Remote Sens. Environ.*, *106*, 238-252.

Lapenis, A., A. Shvidenko, D. Shepaschenko, S. Nilsson, and A. Aiyyer (2005), Acclimation of Russian forests to recent changes in climate, *Global Change Biol.*, *11*, 2090-2102, doi:10.1111/j.1365-2486.2005.01069.x.

Larcher, W. (1995), Physiological Plant Ecology: Ecophysiology and Stress Physiology of Functional Groups, 3rd edition, Springer, New York.

Lescop-Sinclair K. and S. Payette (1995), Recent advance of the Arctic treeline along the east coast of Hudson Bay, *J. Ecol.*, *83*, 929-936.

Liu, H.Q. and A.R. Huete (1995), A feedback based modification of the NDVI to minimize canopy background and atmospheric noise, *IEEE Trans. Geosci. Rem. Sens.*, *33*, 457-465.

Lloyd, A.H. and C.L. Fastie (2002), Spatial and temporal variability in the growth and climate response of treeline trees in Alaska, *Climate Change*, *52*, 481-509.

Lloyd, A.H., and A.G. Bunn (2007), Responses of the circumpolar boreal forest to 20th century climate variability, *Environ. Res. Lett.*, *2*, 045013, doi:10.1088/1748-9326/2/4/045013.

Lopatin, E., T. Kolstrom, H. Spiecker (2006), Determination of forest growth trends in Komi Republic (northwestern Russia): combination of tree-ring analysis and remote sensing data, *Boreal Environ. Res., 11*, 341-353.

McCallum, I., W. Wagner, C. Schmullius, A. Shvidenki, M. Obersteiner, S. Fritz, and S. Nilsson (2009), Satellite-based terrestrial production efficiency modeling, Carbon Balance Manage., 4, doi:10.1186/1750-0680-4-8.

McGuire, A. D., L. G. Anderson, T. R. Christensen, S. Dallimore, L. Guo, D. J. Hayes, M. Heimann, T. D. Lorenson, R. W. Macdonald, and N. Roulet (2009), Sensitivity of the carbon cycle in the Arctic to climate change, *Ecol. Mono., 79,* 523-555.

Montesano, P.M., R. Nelson, G. Sun, H. Margolis, A. Kerber, and K.J. Ranson (2009), MODIS tree cover validation for the circumpolar taiga-tundra transition zone, Remote Sens. Environ., 113, 2130-2114.

Myneni, R.B., F.G. Hall, P.J. Sellers, and A.L. Marshak (1995), The interpretation of spectral vegetation indexes, *IEEE Trans. Geosci. Rem. Sens., 33,* 481-486.

Myneni, R.B., C.D. Keeling, C.J. Tucker, G. Asrar, and R.R. Nemani (1997), Increased plant growth in the northern high latitudes from 1981 to 1991, *Nature, 386,* 697-702.

Nemani, R.R., C.D. Keeling, H. Hashimoto, W.M. Jolly, S.C. Piper, C.J. Tucker, R.B. Myneni, and S.W. Running (2003), Climate-driven increases in global terrestrial net primary production from 1982 to 1999, *Science, 300,* 1560-1562, DOI: 10.1126/science.1082750.

Olthof, I., D. Pouliot, R. Latifovic, and W. Chen (2008), Recent (1986-2006) Vegetation-Specific NDVI Trends in Northern Canada from Satellite Data, *Arctic, 61*, 381-394.

Olthof, I. and Pouliot, D. (2010). Treeline vegetation composition and change in Canada's western Subarctic from AVHRR and canopy reflectance modeling. *Rem. Sens. Environ., 114*, 805-815.

Ostercamp, T.E., L. Viereck, Y. Shur, M.T. Jorgenson, C. Racine, A. Doyle, and R.D. Boone (2000), Observations of Thermokarst and Its Impacts on Boreal Forests in Alaska, U.S.A., *Arctic Antarct. Alpine Res., 32*, 303-315.

Pilcher, J.R. (1990), Sample Preparation, Cross-dating, and Measurement, in *Methods of Dendrochronology*, edited by E.R. Cook and L.A. Kairiukstis, pp. 40-50, Kluwer Academic, Boston.

Prince, S., S. Goetz, and S. Goward (1995), Monitoring primary production from Earth observing satellites, *Water Air Soil Pollut., 82*, 509-522.

Prince S.D. and S.N. Goward (1995), Global primary production: a remote sensing approach, *J. Biogeog., 22*, 815-835.

R Development Core Team (2009), R: A language and environment for statistical computing. R Foundation for Statistical Computing, Vienna, Austria. ISBN 3-900051-07-0, <http://www.R-project.org>.

Rees, G., I. Brown, K. Mikkola, T. Virtanen, and B. Werkman (2002), How can the dynamics of the tundra-taiga boundary be remotely monitored?, *Ambio 12*, 56-62.

Rocha, A.V., M.L. Goulden, A.L. Dunn, and S.C. Wofsy (2006), On linking Interannual tree ring variability with observation of whole-forest CO2 flux, *Global Change Biol., 12*, 1378-1389, doi: 10.1111/j.1365-2486.2006.01179.x.

Romanovsky, V.E., T.S. Sazonova, V.T. Balobaev, N.I. Shender, and D.O. Sergueev (2007), Past and recent changes in air and permafrost temperatures in eastern Siberia, *Global Planet. Change, 56*, 399-413.

Running, S. and E. Hunt (1993), Generalization of a forest ecosystem process model for other biomes, Biome-BGC, and an application for global-scale models, Scaling Physiological Processes, Eds: J. Ehleringer and Field C. San Diego: Academic Press, pg 141-158.

Running, S., P. Thornton, R. Nemani, and J. Glassy (2000), Global terrestrial gross and net primary productivity from the earth observing system, in *Methods in Ecosystem Science*, edited by O. Sala, R. Jackson, H. Mooney, and R. Howarth, pp. 44-55, Springer, New York, U.S.A.

Running, S., R. Nemani, F. Heinsch, M. Zhao, M. Reeves, and H. Hashimoto (2004), A Continuous Satellite-Derived Measure of Global Terrestrial Primary Production, *BioScience, 54*, 547-560.

Schloss, A.L., D.W. Kicklighter, J. Kaduk, U. Wittenberg and the Participants of the Postsdam NPP Model Intercomparison (1999), Comparing global models of terrestrial net primary productivity

(NPP): comparisons of NPP to climate and the Normalized Difference Vegetation Index (NDVI), *Global Change Biol., 5*, 25-34.

Steven, M.D., T.J. Malthus, F. Baret, H. Xu, and M.J. Chopping (2003), Intercalibration of vegetation indices from different sensor systems, *Rem. Sens. Environ., 88*, 412-422.

Stocks, B. J., J. A . Mason, J. B. Todd, E. M. Bosch, B. M. Wotton, B. D. Amiro, M.D. Flannigan, K.G. Hirsch, K.A. Logan, D.L. Martell, W.R. Skinner (2002), Large forest fires in Canada, 1959–1997. *J. Geophys. Res., 107*, doi:10.1029/2001JD000484.

Stoy, P.C., M. Williams, M. Disney, A. Prieto-Blanco, B. Huntley, R. Baxter, and P. Lewis (2009), Upscaling as ecological information transfer: a simple framework with application to Arctic ecosystem carbon exchange, *Landscape Ecol., 24,* 971-986. DOI 10.1007/s10980-009-9367-3.

Sukhinin A.I., N.H.F. French, E.S. Kasischke, J.H. Hweson, A.J. Soja, I.A. Csiszar, E.J. Hyer, T. Loboda, S.G. Conrad, V.I. Romasko, E.A. Pavlichenko, S.I. Miskiv, and O.A. Slinkina (2004), AVHRR-based mapping of fires in Russia: New products for fire management and carbon cycle studies. *Remote Sens. Environ.*, 93, 546-564.

Suzuki, R., S. Tanaka, and T. Yasunari (2000), Relationships between meridional profiles of satellite-derived vegetation index (NDVI) and climate over Siberia, *Int. J. Climate., 20,* 955-967.

Tape, K., M. Strum and C. Racine (2006), The evidence for shrub expansion in Northern Alaska and the Pan-Arctic, *Global Change Biol., 12*, 686-702, doi: 10.1111/j.1365-2486.2006.01128.x.

Tarnocai, C., J.G. Canadell, E.A.G. Schuur, P. Kuhry, G. Mazhitova, and S. Zimov (2009), Soil organic carbon pools in the northern circumpolar permafrost region, Global Change Biol., 23, GB2023, doi:10.1029/2008GB003327.

Thompson, J.N., O.J. Reichman, P.J. Morin, G.A. Polis, M.E. Power, R.W. Sterner, C.A. Couch, L. Gouch, R. Holt, D.U. Hooper, F. Keesing, C.R. Lovell, B.T. Milne, M.C. Molles, D.W. Roberts, and S.Y. Strauss (2001), Frontiers of Ecology, *BioScience, 51*, 15-24.

Tucker, C.J. (1979), Red and photographic infrared linear combinations for monitoring vegetation, *Rem. Sens. Environ., 8*, 127-150.

Tucker, C.J., I.Y. Fung, C.D. Keeling and R.H. Gammon (1986), Relationship between atmospheric CO2 variations and a satellite-derived vegetation index, *Nature, 319,* 195-199.

Tucker, C. J., J.E. Pinzon, M.E. Brown, D. Slayback, E.W. Pak, R. Mahoney, E. Vermote, and N. El Saleous (2005), An extended AVHRR 8-km NDVI Data Set Compatible with MODIS and SPOT Vegetation NDVI Data. *Int. J. Rem. Sens., 26*, 4485−4498.

Turner, M.G., R.V. O'Neill, R.H. Gardner, and B.T. Milne (1989), Effects of changing spatial scale on the analysis of landscape pattern, *Landscape Ecol., 3*, 153-162.

Turner, M. (2005). Landscape Ecology: What is the State of the Science?. *Annu. Rev. Ecol. Evol. Syst., 36,* 319-344.

Vygodskaya, N.N., P.Y. Groisman, N.M. Tchebakova, J.A. Kurbatova, O.P. Panfyorov, E.I. Parfenova, and A.F. Sogachev (2007), Ecosystem and climate interactionsin the boreal zone of northern Eurasia, *Environ. Res. Lett., 2*, 045033, doi:10.1088/1748-9326/2/4/045033.

Wallin, D.O., C.C.H. Elliott, H.H. Shugart, C.J. Tucker and F. Wilhelmi (1992), Satellite remote sensing of breeding habitat for an African weaver-bird, *Landscape Ecol., 7*, 87-99.

Wang, J., P.M. Rich, K.P. Price, and W.D. Kettle (2004), Relations between NDVI and tree productivity in the central Great Plains, *Int. J. Rem. Sens., 25*, 3127-3138.

Wiens, J.A. (1989). Spatial Scaling in Ecology, *Function. Ecol.*, 3, 385-397.

Zhang, X., M. A. Friedl, C. B. Schaaf, A. H. Strahler, J. C. F. Hodges, F. Gao, B. C. Reed, and A. Huete (2003), Monitoring vegetation phenology using MODIS, *Rem. Sens. Environ., 84*, 471-475.

Zhang, K., J. S. Kimball, K.C. McDonald, J. J. Cassano, and S. W. Running (2007), Impacts of large-scale oscillations on pan-Arctic terrestrial net primary production, *Geophys. Res. Lett., 34*, L21403, doi:10.1029/2007GL031605.

Zhang, K., J. S. Kimball, E. H. Hogg, M. Zhao, W.C. Oechel, J.J. Cassano, and S.W. Running (2008), Satellite-based model detection of recent climate-driven changes in northern high-latitude vegetation production, *J. Geophys. Res., 113*, G03033, doi:10.1029/2007JG000621.

Zhou, L., C.J. Tucker, R.K. Kaufmann, D. Slayback, N.V. Shabanov, and R.B. Myneni (2001), Variations in northern vegetation activity inferred from satellite data of vegetation index during 1981 to 1999, *J. Geophys. Res., 106,* 20069-20083.

Zimov, S.A., Y.V. Voropaev, I.P. Semiletox, S.P. Davidov, S.f. Prosiannikov, F.S. Chapin III, M.C. Chapin, S. Trumbore, and S. Tyler (1997), North Siberian Lakes: A Methane Source Fueled by Pleistocene Carbon, *Science, 277,* 800-802, DOI: 10.1126/science.277.5327.800.

Zimov, S.A., E.A.G. Schuur, and F.S. Chapin III (2006), Permafrost and the Global Carbon Budget, *Science, 312,* 1612-1613.

APPENDICES

A.1. **Tree Ring Measurements and Chronology Statistics**

Table A-1. Tree ring measurements and chronology statistics for the 27 tree ring chronologies collected in Canada and Russia during 2008 and 2009. Abbreviations: I.C. = Interseries Correlation, A.C. = Autocorrelation, M.S. = Mean Sensitivity.

Genus	Site	Series				Measurements (mm)			Chronology Metrics		
		Trees	Start Year	End Year	Mean Length	Mean	Max	Std	I.C.	A.C.	M.S.
Larix	CHE	57	1718	2007	171.6	0.53	9	0.349	0.713	0.785	0.332
	DVN	9	1840	2007	102.6	0.94	3.5	0.631	0.762	0.807	0.332
	GRS	13	1805	2007	131.4	0.77	3.61	0.427	0.8	0.675	0.346
	IND	25	1519	2007	257.5	0.57	3.48	0.342	0.515	0.725	0.327
	PAR	13	1828	2007	88.5	1	4.03	0.61	0.762	0.744	0.347
	ROD	14	1835	2007	107.7	0.72	3.49	0.535	0.776	0.8	0.343
	SYL	24	1719	2007	153.5	0.84	3.67	0.494	0.665	0.793	0.293
	TRL	7	1821	2007	96	0.54	2.7	0.296	0.681	0.636	0.35
	YUT	30	1797	2007	147.8	0.9	4.36	0.442	0.62	0.751	0.258
	ZHG	60	1960	2007	47.7	0.69	5.81	0.369	0.65	0.612	0.33
Picea	BIS	10	1933	2008	57.1	1.18	3.86	0.76	0.524	0.895	0.207
	FAL	8	1819	2008	148.1	0.46	2.45	0.247	0.545	0.862	0.183
	NML	21	1903	2008	69.9	1.78	4.98	0.532	0.741	0.678	0.188
	DAR	10	1909	2008	64.9	1.38	4.85	0.536	0.661	0.627	0.242
	ELF	5	1943	2008	58.1	1.92	4.16	0.768	0.703	0.756	0.169
	FAH	19	1824	2008	78.7	0.98	5.22	0.593	0.526	0.919	0.177
	SQT	22	1903	2008	89.2	1.15	5.6	0.733	0.691	0.925	0.17
	TAL	8	1929	2008	56.9	0.95	2.55	0.356	0.567	0.711	0.182
	IND	8	1960	2007	48	1.11	5	0.493	0.544	0.685	0.222
	ZHF	10	1695	2007	204.9	0.34	4.55	0.279	0.581	0.801	0.294
Pinus	DAR	14	1894	2008	91.5	0.89	3.63	0.535	0.621	0.816	0.268
	ELF	16	1922	2008	76	1.6	7.52	1.285	0.574	0.903	0.205
	FAL	10	1816	2008	110.9	0.61	3.18	0.434	0.592	0.885	0.222
	MAR	23	1852	2008	89.1	0.7	3.48	0.388	0.612	0.815	0.247
	MKZ	18	1951	2008	52.6	1.34	5.66	1.097	0.658	0.935	0.218
	TAL	14	1899	2008	78.6	0.71	3.09	0.393	0.677	0.753	0.282
	BAL	31	1810	2007	155.6	0.64	3.43	0.373	0.685	0.794	0.256

A.2. **NDVI-RWI Correlation Coefficients**

Table A-2. Pearson's correlation coefficients assessing the relationship between AVHRR-derived NDVI and ring width indices for 27 chronologies over the 1982 to 2008 period. N_{eff} is the effective sample size used when determining correlation significance and was reduced from the initial N based on the strength of the NDVI or RWI autocorrelation. [a] canopy, codominance, ** $p \leq 0.05$, * $p \leq 0.10$

Genus	Site	N_{eff}	r
Larix	CHE	26	0.33*
	DVN	26	0.43**
	GRS	26	0.57**
	IND[a]	26	0.32
	PAR	26	0.08
	ROD	26	0.40**
	SYL	26	0.32
	TRL	26	0.45**
	YUT	26	0.27
	ZHG	26	0.67**
Picea	BIS	8	0.51
	FAL[a]	12	0.34
	NML	15	0.39
	DAR[a]	26	0.31
	ELF[a]	10	0.44
	FAH	6	0.75**
	SQT	11	0.68**
	TAL[a]	13	0.62**
	IND[a]	26	0.16
	ZHF	26	0.28
Pinus	DAR[a]	26	0.15
	ELF[a]	12	0.36
	FAL[a]	9	-0.58*
	MAR	11	0.59*
	MKZ	9	0.82**
	TAL[a]	15	0.62**
	BAL	26	0.36*

A.3. **NDVI-RWI Time-Series Moving Average**

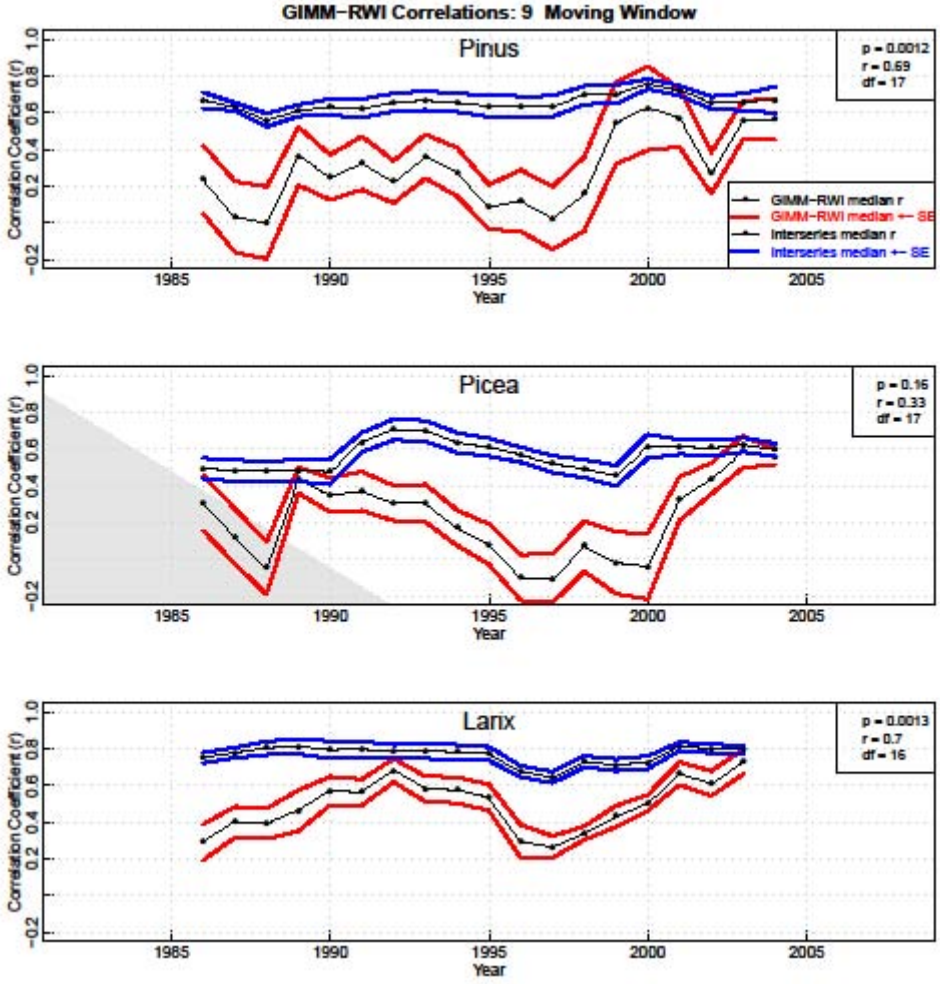

Figure A-3. Time series plots showing nine year moving-window NDVI-RWI correlations and median chronology interseries correlations for *Larix*, *Pinus*, and *Picea*. Interseries correlations denote the extent to which trees in a stand exhibit synchronicity in growth. The agreement between both sets of correlations is also shown for each genus. While the time series is too short to conduct a robust analysis, these figures suggest that the strength of the NDVI-RWI correlations may change with time and that the changes may occur at points where interseries correlations also change. A longer time series will be necessary before it will be possible to formally conduct such an analysis.

A.4. **MODIS and AVHRR NDVI Correlation by Land**

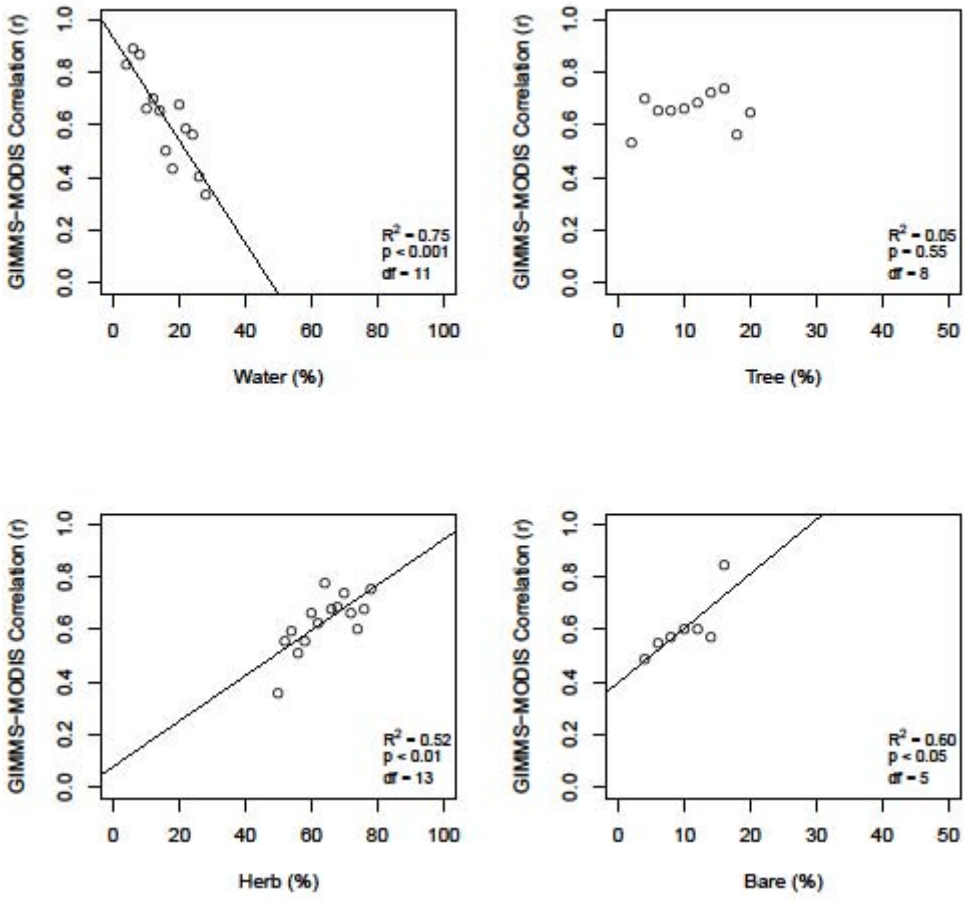

Figure A-4. Initial attempts were made to examine the agreement between MODIS and AVHRR NDVI products as a function of land cover. These data are for a 400 km x 300 km region along the taiga-tundra boundary in the Northwest Territories during July of 2007. Each dot represents the correlation coefficient (r) relating between 30 and a few hundred GIMMS and MODIS pixels that were binned into 5%, non-overlapping subsets based on the land cover composition. Land cover was determined using the VCF product. Regression lines were then added when significant relations were observed. These preliminary findings suggest that the sensors show the highest agreement in areas of low water cover and high herb cover.